Quaternary Science Reviews 134 (2016) 74–91

Contents lists available at ScienceDirect

Quaternary Science Reviews

journal homepage: www.elsevier.com/locate/quascirev

Glacial chronology and palaeoclimate in the Bystra catchment, Western Tatra Mountains (Poland) during the Late Pleistocene

Michał Makos [a, *], Vincent Rinterknecht [b, c], Régis Braucher [d], Michał Żarnowski [a], Aster Team[d, 1]

[a] Climate Geology Department, University of Warsaw, 93 Żwirki i Wigury St., 02-089 Warsaw, Poland
[b] Université Paris 1 Panthéon-Sorbonne, Laboratoire de Géographie Physique, CNRS, UMR 8591, 92195 Meudon, France
[c] School of Geography and Geosciences, University of St Andrews, KY16 9AL St Andrews, UK
[d] Aix-Marseille Université, CNRS-IRD-Collège de France, UMR 34 CEREGE, Technopôle de l'Environnement Arbois-Méditerranée, BP80, 13545 Aix-en-Provence, France

ARTICLE INFO

Article history:
Received 4 October 2015
Received in revised form
8 January 2016
Accepted 11 January 2016
Available online 21 January 2016

Keywords:
10-Be chronology
Deglaciation
Palaeoclimate
Late Pleistocene
Tatra Mountains

ABSTRACT

Deglaciation chronology of the Bystra catchment (Western Tatra Mountains) has been reconstructed based on ^{10}Be exposure age dating. Fourteen rock samples were collected from boulders located on three moraines that limit the horizontal extent of the LGM maximum advance and the Lateglacial recessional stage. The oldest preserved, maximum moraine was dated at 15.5 ± 0.8 ka, an age that could be explained more likely by post-depositional erosion of the moraine. Such scenario is supported by geomorphologic and palaeoclimatological evidence. The younger cold stage is represented by well-preserved terminolateral moraine systems in the Kondratowa and Sucha Kasprowa valleys. The distribution of the moraine ridges in both valleys suggest a complex history of deglaciation of the area. The first Late-glacial readvance (LG1) was followed by a cold oscillation (LG2), that occurred at around 14.0 ± 0.7–13.7 ± 1.2 ka. Glaciers during both stages had nearly the same horizontal extent, however, their thickness and geometry changed significantly, mainly due to local climatic conditions triggered by topography, controlling the exposition to solar radiation. The LG1 stage occurred probably during the pre-Bølling cold stage (Greenland Stadial 2.1a), however, the LG2 stage can be correlated with the cooling at around 14 ka during the Greenland Interstadial 1 (GI-1d – Older Dryas). This is the first chronological evidence of the Older Dryas in the Tatra Mountains. The ELA of the maximum Bystra glacier was located at 1480 m a.s.l. in accordance with the ELA in the High Tatra Mountains during the LGM. During the LG1 and LG2 stages, the ELA in the catchment rose up to 1520–1530 m a.s.l. and was located approximately 100–150 m lower than in the eastern part of the massif. Climate modelling results show that the Bystra glacier (maximum advance) could have advanced in the catchment when mean annual temperature was lower than today by 11–12 °C and precipitation was reduced by 40–60%. This is in accordance with LGM conditions previously reported for the High Tatras. During the LG1 and LG2 stages the temperature decrease in the study area reached 10 °C and precipitation was lower by ~30% compare to modern conditions. This resulted in slightly higher accumulation (20–30%) in the Western Tatra Mountains compare to the High Tatra Mountains.

1. Introduction

Quantifying environmental and palaeoclimatological fluctuations in mountains of central Europe during the last glacial cycle is crucial in order to understand the prevailing atmospheric circulation patterns in a relatively sensitive area located between the Scandinavian Ice Sheet and the Alpine Ice Cap (Heyman et al., 2013). Recent studies on paleogeography and climate during the last glaciation have been carried out in e.g. Central European Uplands (Heyman et al., 2013; Mentlik et al., 2013; Engel et al., 2014) and High Tatra Mountains (Makos et al., 2014; Makos, 2015; Engel

* Corresponding author.
E-mail address: michalmakos@uw.edu.pl (M. Makos).
[1] Maurice Arnold (arnold@cerege.fr), Georges Aumaître (aumaitre@cerege.fr), Didier Bourlès (bourles@cerege.fr), Karim Keddadouche (keddadouche@cerege.fr).

http://dx.doi.org/10.1016/j.quascirev.2016.01.004
0277-3791/

et al., 2015). Paleoglaciological investigations combined with studies on chronology of glacial episodes in mountains of Europe give the opportunity for reconstructing the principal climatic parameters (temperature and precipitation) during specific periods when glaciers were stable. Assuming the sensitivity of glacial systems, especially mountain glaciers, for even slight climatic fluctuations, it is possible to follow the successive environmental changes during the process of deglaciation, when series of recessional moraines have been formed. Combination of dating technique using cosmogenic nuclides and glacier-climate modelling allow to identify the timing and the strength of cold events and to correlate events across different regions. Cosmogenic isotopes have been used for chronological studies in many mountain ranges in Europe e.g.: Alps (Ivy-Ochs et al., 2008, 2009), Pyrenees (Delmas et al., 2011; Palacios et al., 2015), Scottish Highlands (Ballantyne, 2010; Small et al., 2012), Carpathians (Reuther et al., 2007; Rinterknecht et al., 2012; Makos et al., 2013a,b; 2014; Kuhlemann et al., 2013; Engel et al., 2015), Dinarides (Hughes et al., 2010, 2011), Rila Mountains (Kuhlemann et al., 2013).

According to the Greenland ice -core chronology, several significant climatic fluctuations are observed in the Northern Atlantic region during the Late Pleistocene, within the time range of 26–11.7 ka (Björk et al., 1998; Lowe et al., 2008; Rasmussen et al., 2014). These episodes left a significant geomorphologic imprint in many mountain ranges across Europe where exposure age chronologies correlate well with the North Atlantic climatic events (González-Sampériz et al., 2006; Kuhlemann et al., 2008, 2009; Delmas et al., 2008; Sarikaya et al., 2008, 2009; Federici et al., 2012; Darnault et al., 2012; Engel et al., 2014, 2015; Makos et al., 2013, 2014).

The most significant cooling during the last glacial cycle, the Last Glacial Maximum (LGM), took place between 26.5 and 19 ka (Clark et al., 2009). This episode is recorded as a worldwide drop in a mean sea level of ~120 m (Peltier and Fairbanks, 2006). The temperature decrease in Central European lowlands could have reached 5–10 °C, while in mountainous area it could have reached 17 °C with attendant reduction of precipitation between 50 and 70% (Allen et al., 2008; Strandberg et al., 2011). In the Tatra Mountains the annual temperature and precipitation were decreased by 11–12 °C and at least 40–60%, respectively (Makos et al., 2014).

Following the LGM, glaciers in the mountains of Europe retreated rapidly. This episode defined as the LG ice decay was the most prominent within large ice caps such as the Alpine ice cap, which lost 80% of its volume before 18 ka (Ivy-Ochs et al., 2008). During the LG at least few glacier oscillations are recorded across Europe from the Pyrenees (Delmas et al., 2011) to the Anatolian Peninsula (Sarikaya et al., 2008). These glacial episodes correlate well with climatic events recorded in the Greenland ice core (Lowe et al., 2008; Rasmussen et al., 2014). The first post-LGM oscillation of the Alpine glaciers occurred during the Greenland Stadial 2c around 21.2–19.5 ka (Reitner, 2007). Glaciers were stable again during the Greenland Stadial 2b around 18 ka, when the first post-maximum recessional moraines were formed in the Rila Mountains (Kuhlemann et al., 2013) and the Tatra Mountains (Makos et al., 2014).

Further glacial oscillations in Europe, well-documented in the Alps (Ivy-Ochs et al., 2006, 2008; Federici et al., 2012; Darnault et al., 2012), the Carpathians (Reuther et al., 2007; Makos et al., 2013a) and the Pyrenees (Delmas et al., 2008), took place during Greenland Stadial 2.1a (the Oldest Dryas) at 17–15 ka. In the Central Alps the final stabilization of ice front during the Gschnitz Stadial occurred at around 15.7 ka when the summer precipitation was lower than today by about 10 °C (Ivy-Ochs et al., 2006). In the Tatra Mountains the drop of annual temperature reached 9–10 °C (Makos et al., 2013a). Independent data from lacustrine sediments confirm a significant cooling by about 8 °C in the Swiss Alps (Larocque-Tobler et al., 2010) and around 6 °C in Northern Romania (Feurdean et al., 2008). The undoubtedly cold Oldest Dryas (OD) took place when the North Atlantic Oscillation changed during Heinrich Event 1 (Hemming, 2004).

The Younger Dryas (YD) was the last major cold event in Europe (Isarin and Renssen, 1999; Broecker, 2006) and correspond to the Greenland Stadial 1. Many mountain glaciers in Europe advanced markedly around 13–12 ka (Delmas et al., 2008; Kuhlemann et al., 2009; Ivy-Ochs et al., 2009; Rinterknecht et al., 2012; Makos et al., 2013b). The alpine Egesen Stadial was characterized by 5 °C lower summer temperature and about 30% lower precipitation. In the Tatra Mountains these climatic parameters were lower by 4.5 °C and 25%, respectively (Makos et al., 2013b). The pollen-based mean annual temperature in NW Romania dropped by about 5 °C (Feurdean et al., 2008), while the glacier-climate model from the High Tatras confirm a 6–7 °C decrease (Makos et al., 2013b). Because the temperature change across Europe during the Younger Dryas was rather similar, the precipitation could have played a determining role in the glacier mass balance.

Studies on glacial history of the Tatra Mountains have been carried on for over 200 years (Klimaszewski, 1988 and reference therein). Over that time period many ideas were presented and their evolution has been paralleled with progresses in research methodologies. Based on geomorphologic analysis of fluvioglacial sediments in the Tatra's foreland, Lindner et al. (2003) distinguished eight glacial cycles in the massif during the Pleistocene. Their conclusions were based mainly on the thermoluminescence dating of fluvioglacial deposits. The same methodology gave the opportunity to divide the last glacial cycle (Würm) into three stadials and the last stadial into four phases (Lindner et al., 2003). At the end of twentieth century, exposure age dating using ^{36}Cl was applied for the first time in the High Tatra Mountains (Dzierżek et al., 1999). Development of the deglaciation chronology of the last glacial cycle continued mainly in the eastern part of the mountain chain (Dzierżek, 2009; Makos and Nitychoruk, 2011; Makos et al., 2013a and b; 2014; Engel et al., 2015). The most extensive terminal moraines were formed during the global LGM at around 26–21 ka (Makos et al., 2014). Following the global LGM, at least four glacier oscillations occurred at around 18 ka, 17–16 ka, 15 ka and 12,5 ka (Makos et al., 2013a and b; 2014; Makos, 2015; Engel et al., 2015). Older glacial cycles are probably represented by highly weathered deposits in the foreland of the LGM moraines (Klimaszewski, 1988; Baumgart-Kotarba and Kotarba, 1997).

The aim of this study is to introduce the reconstruction of the LG deglaciation pattern and its palaeoclimatic implications in the Bystra catchment located in the Polish sector of the Western Tatra Mountains. Our chronology and modelling results together with already published data allow to assess the palaeoclimatic regimes of the Western Tatras and the High Tatras (eastern part of the massif). The chronology of glacial episodes in the study area has been carried out based on ^{10}Be exposure dating, which was implemented for the first time in the Polish Tatra Mountains.

2. Study area

2.1. Geology and geomorphology

The Tatra Mountains are the highest massif of the Carpathians (Gerlachovský Štit - 2655 m a.s.l.) located on the Polish - Slovakian border (Fig. 1). They were strongly glaciated during the Pleistocene with large valley glaciers on both southern and northern side of the chain (Zasadni and Kłapyta, 2014). The Bystra catchment is located in the Polish part of the Western Tatra Mountains (49°250611N; 19.971455E) and its formerly glaciated area extends between the

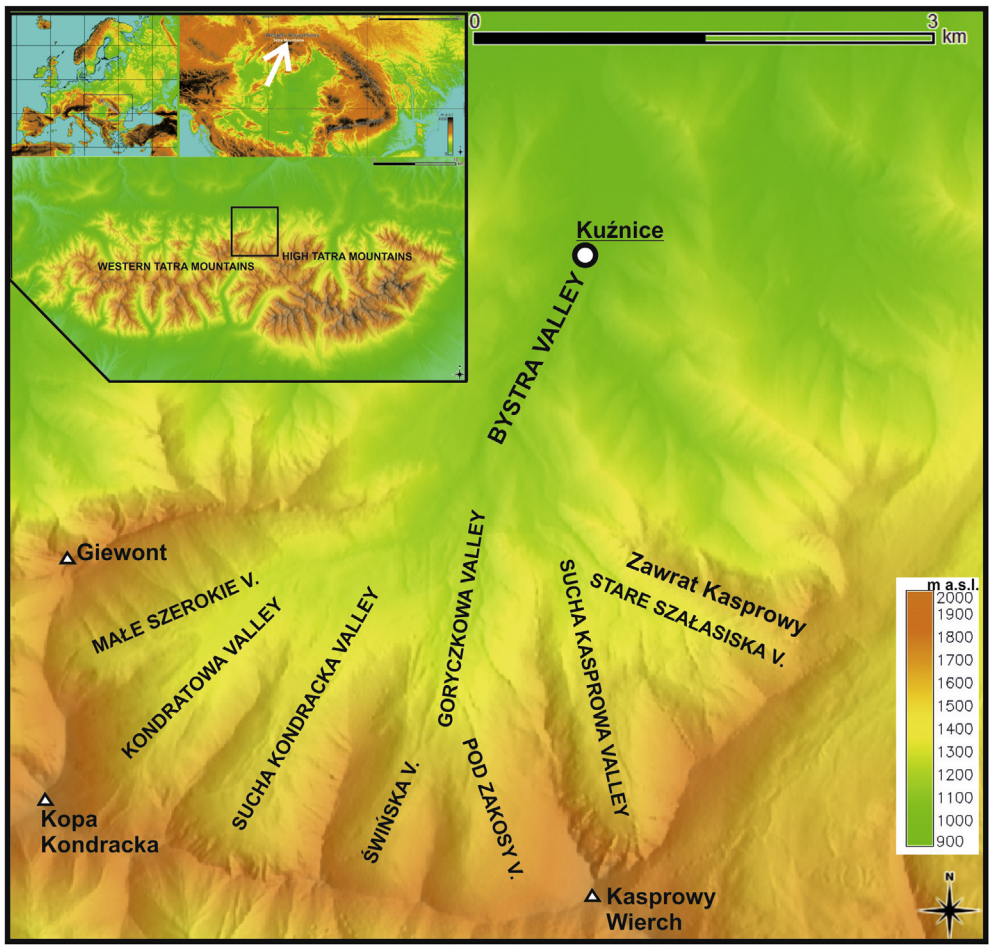

Fig. 1. Location of the study area. White arrow shows location of the Tatra Mountains in the Carpathians chain.

maximum moraine at 1020 m a.s.l. and the cirque headwalls at ~1800 m a.s.l (Fig. 1). The drainage basin covers an area of 16.5 km^2 and is composed of the main Bystra Valley and four tributaries: Kondratowa Valley, Sucha Kondracka Valley, Goryczkowa Valley and Sucha Kasprowa Valley. All four tributaries are incised within the crystalline and metamorphic granites as well as gneisses, which comprise the central part of the Giewont nappe. These granites form a klippe, covering the younger sedimentary rocks, which are exposed in the lower part of the catchment, mainly within the Bystra Valley. The sedimentary set is composed of Trassic and Jurassic very hard and resistant massive limestones and dolomites (upper nappe). The latter build a narrow zone between the crystalline klippe and Triassic and Jurassic soft dolomites and shales (lower nappe) located in the lowermost part of drainage basin. The valleys and cirques are draped with glacially transported material, which consists of crystalline and metamorphic granites and gneisses from the Giewont nappe.

An extensive part of the Bystra Valley is covered with ground moraine/till. In the north, the extent of the glaciated area is limited by a prominent end moraine (30 m high) terminating at 1020 m a.s.l. (Fig. 2). The eastern and western segments of this end moraine are continuous over ~1500 m and reach the level of 1200 m a.s.l. as lateral moraines. This termino-lateral moraine system represents a clear constraint for the former glacier geometry reconstruction. The younger morphostratigraphic unit is located ~1300 m up-valley from the end moraine. Two well-formed terminal moraines were deposited at the mouths of the Sucha Kasprowa and Kondratowa/Sucha Kondracka valleys. The moraines are located at the level of 1250 m a.s.l. (Fig. 2).

The termino-lateral moraine system in the Sucha Kasprowa Valley is 20 m high, forms as a single ridge, and is continuous from the terminal part up to the elevation of 1370 m a.s.l. The lateral segment of this moraine was only preserved on the eastern side of the valley (Fig. 2). The whole feature is composed of granitic boulders with long axis up to 3 m and located on the moraine crest.

The terminal moraine in the Kondratowa/Sucha Kondracka Valley has a steep and high distal slope (up to 50 m). The highest outer ridge is very well-preserved, composed of big boulders up to 3 m long. The inner part of moraine is composed of many small ridges and hollows, probably reflecting aerial downwasting of the glacier's snout. Deposits of the terminal moraine cover the area between 1250 and 1300 m a.s.l. There is another lateral moraine ridge in the lowermost part of the Kondratowa Valley. This 20 m high moraine is located between 1300 and 1350 m a.s.l. and was formed between two downwasting tongues of the Kondratowa and the Sucha Kondracka glaciers (Fig. 2).

Younger glacial activity is recorded in the uppermost part of Sucha Kondracka and Sucha Kasprowa valleys. Both valleys end up as glacial cirques fully covered by rock debris reworked by periglacial activity (Fig. 2). The elongated and spoon-shaped ridges and hollows indicate the former activity of a rock glacier. At present these forms are no more active, thus they are described as fossil rock glaciers. In the Sucha Kondracka cirque the rock glacier covers an area of 0.27 km^2 between 1550 and 1400 m a.s.l. It is located on

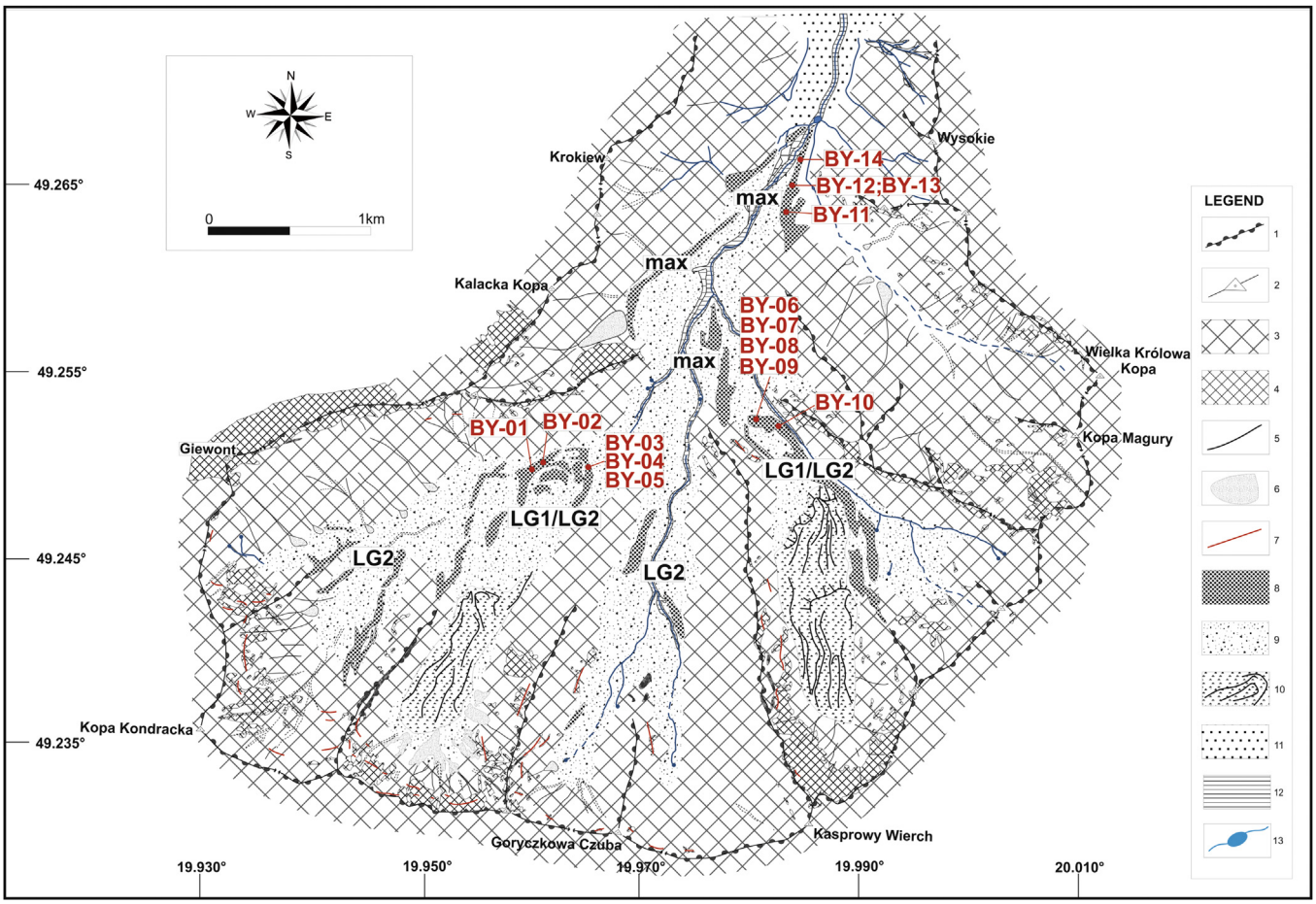

Fig. 2. Geomorphological map of the Bystra catchment (based on Żarnowski, 2015 - modified): 1 – crests and arêtes; 2 – summits; 3 – valley and cirque slopes covered with debris and vegetation; 4 – steep rock walls; 5 – gullies; 6 – talus cones; 7 – glacial trimlines; 8 – terminal and lateral moraine ridges; 9 – ground moraines; 10 – fossil rock glaciers; 11 – fluvioglacial plains; 12 – fluvial terraces; 13 – rivers and lakes. Red dots mark location of the samples.

the flat valley floor and its upper margin is limited by vast talus cones covering the headwall of the cirque. In the Sucha Kasprowa cirque the extent of fossil rock glacier reaches of 0.42 km^2. It covers the valley floor between 1600 and 1300 m a.s.l. The longitudinal profile of the cover shows a very significant step at the elevation of 1500 m a.s.l. This step reflects the younger front of the rock glacier. Therefore, there were most likely two phases of periglacial activity in the valley. An older one with the front at 1300 m a.s.l. and a younger one at 1500 m a.s.l. There are no glacial erosional forms preserved on the valley floor. However, poorly preserved glacial trimlines were mapped on the glacial cirque walls (Fig. 2). In the Bystra catchment, the mapped trimlines are formed mainly as clear steps on the slope, separating a steeper slope below from a gentler slope above. There are no signs of glacial polishing or moulding visible. Glacial trimlines are slightly inclined towards the mouth of the valley with respect to the slope of the cirque floors and reflect the decreasing surface of the glaciers. We assume that the upper part of the trimline (rock step) is the upper limit of the active eroding glacier (Kelly et al., 2004; Fabel et al., 2012; Makos et al., 2013a).

2.2. Climate

The Tatra Mountains are located in the zone of influence of several air masses. The prevailing polar-oceanic air masses come into central Europe from the northern Atlantic Ocean and bring a large amount of precipitation. The other, less important direction of air masses inflow is from north-east, bringing very dry air and being responsible for cooling in winter and warming in summer. Such diversity, with very unstable weather during the year, determines the general climatic conditions in the Tatra Mountains, and is characteristic for a temperate climate zone (Niedźwiedź, 1992).

In this study we used the data from meteo stations in Zakopane (850 m a.s.l.) and in Kasprowy Wierch (1991 m a.s.l.) as well as from temporal meteo sites (precipitation) located in the Bystra catchment: Kalatówki (1195 m a.s.l.) and Myślenickie Turnie (1360 m a.s.l.) (IMGW-PIB (CBDH), www.imgw.pl; National Climatic Data Center, www.ncdc.noaa.gov) (Fig. 3). The data set from the period between years 1955 and 2000 provides a mean annual temperature range from around 6 °C in the Tatras foreland to −4 °C on the highest peaks. In Zakopane, the mean annual temperature is 6.4 °C and the mean summer temperature (June, July, August) is 14 °C. At the Kasprowy Wierch station these values are −0.5 °C and 7.2 °C, respectively. Together these values give a vertical temperature gradient of 0.6 °C/100 m (Fig. 3). The precipitation distribution is more diverse and less linear compare to the temperature distribution. We observe higher gradients between 800 m a.s.l. and 1600 m a.s.l. (100 mm/100 m), while above the elevation of 1700 m a.s.l. the precipitation gradient on the northern slope of the Tatra Mountains is negative. Such situation is determined by the mean level of the cloud base during the year (Niedźwiedź, 1992). The

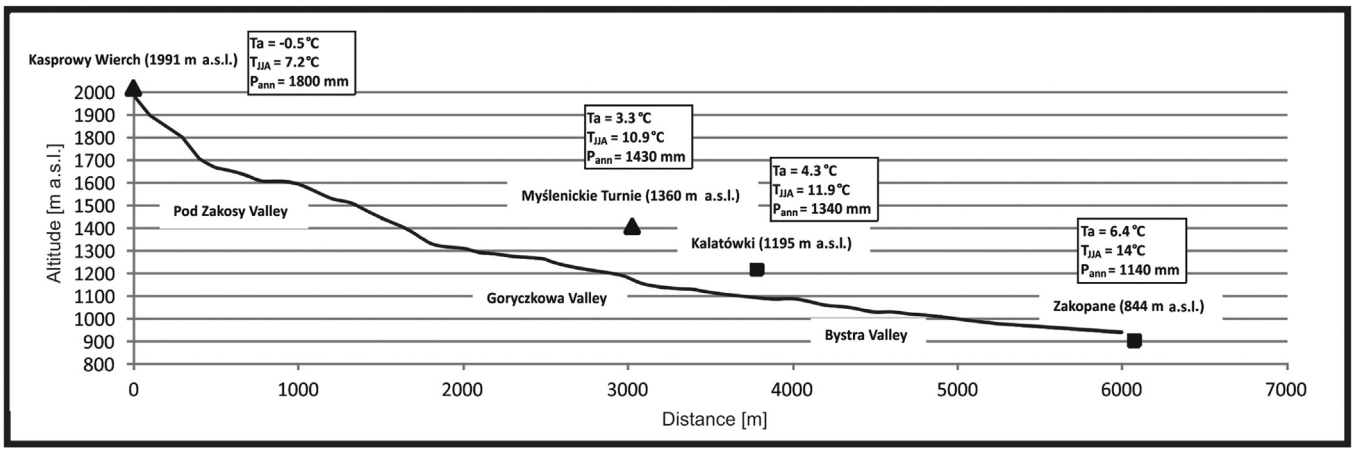

Fig. 3. Distribution of the present-day climatic parameters along the longitudinal profile of Bystra catchment. The data were used in glacier-climate modelling.

precipitation data set from the study area indicates that the annual precipitation increases from 1140 mm in Zakopane (850 m a.s.l.) to 1340 mm and 1430 mm in Kalatówki (1195 m a.s.l.) and Myślenickie Turnie (1360 m a.s.l.), respectively; and up to 1800 mm in Kasprowy Wierch (1991 m a.s.l.) (Fig. 3). We calculated a mean vertical precipitation gradient of ~64 mm/100 m, a value used for our glacier-climate modelling. The snow cover thickness and its preservation is directly proportional to the annual temperature and precipitation. The mean number of days with snow cover varies from 124 in Zakopane through 186 in Hala Gąsienicowa (1520 m a.s.l.) up to 222 in Kasprowy Wierch.

3. Methodology

3.1. Surface exposure dating

3.1.1. Boulder collections

We collected 14 samples in the Bystra Valley on three different moraines: four on the maximum moraine (samples BY-11 to BY-14), five on the Kondratowa LG1 moraine (samples BY-01 to BY-05), and five on the Sucha Kasprowa LG1 moraine (samples BY-06 to BY-10) (Fig. 4–6, Table 1). We sampled the largest boulders available at the surface of the moraines, representing the best stable erratics available for surface exposure dating. We systematically sampled the top flat surface with a manual jackhammer assuming that the boulder top was exposed to secondary cosmic ray since deposition of the boulder at the front of the ice margin (Figs. 4 and 5). Sample coordinates and elevations were recorded with a hand held GPS receiver and shielding by surrounding mountain slopes was recorded using a compass and a clinometer. All sampled boulders are composed of granite with a quartz content ranging between 40% and 50%.

3.1.2. Sample preparation and analysis

All samples were crushed and sieved in order to isolate the 250–1000 μm fraction, which was subsequently decontaminated by successive acid leaching (HCl + H_2SiF_6 then dilute HF). Purified quartz was spiked with ~100 μl of a 3025 ppm home-made carrier then dissolved in 48% HF. Beryllium was complexed by acetyl acetone in a 50% EDTA solution then extracted using solvent extraction. Beryllium hydroxides were dried and oxidized at 800 °C to BeO. Beryllium oxide was mixed to 325 mesh niobium powder prior its measurement at ASTER the French Accelerator Mass Spectrometer located at CEREGE, Aix-en-Provence. Data were normalized directly against the National Institute of Standards and

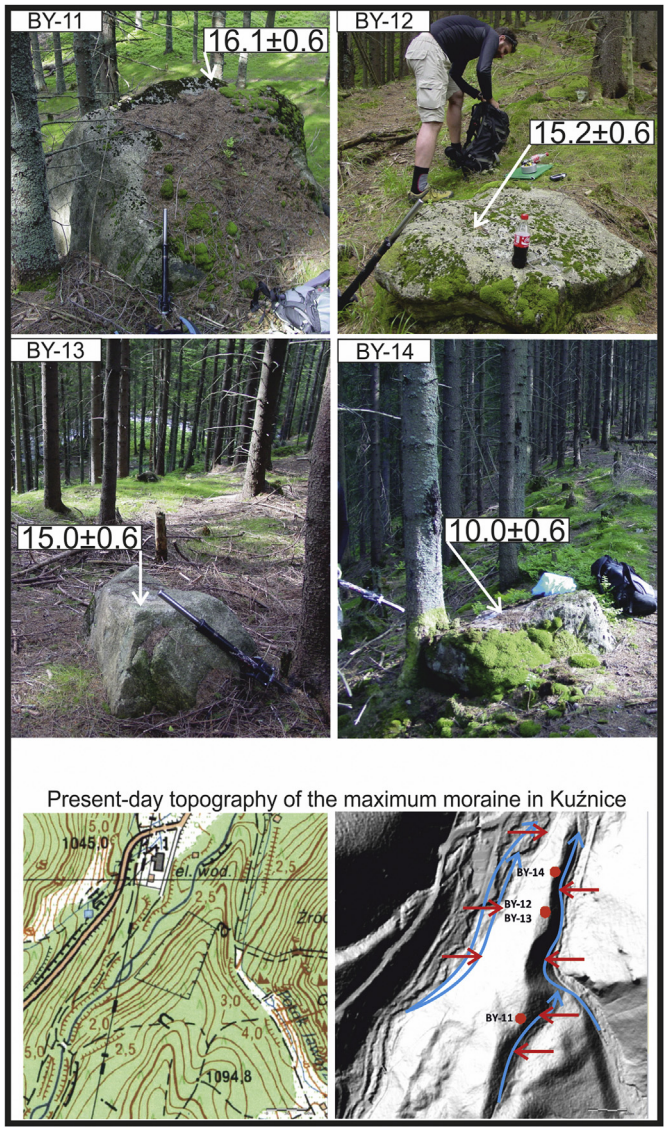

Fig. 4. Sampled boulders on the maximum moraine in Kuźnice. The present-day topography of the moraine indicates its steep morphology. Blue arrows show the direction of eroding water flow. Red arrows show locations of the evidenced river cuts.

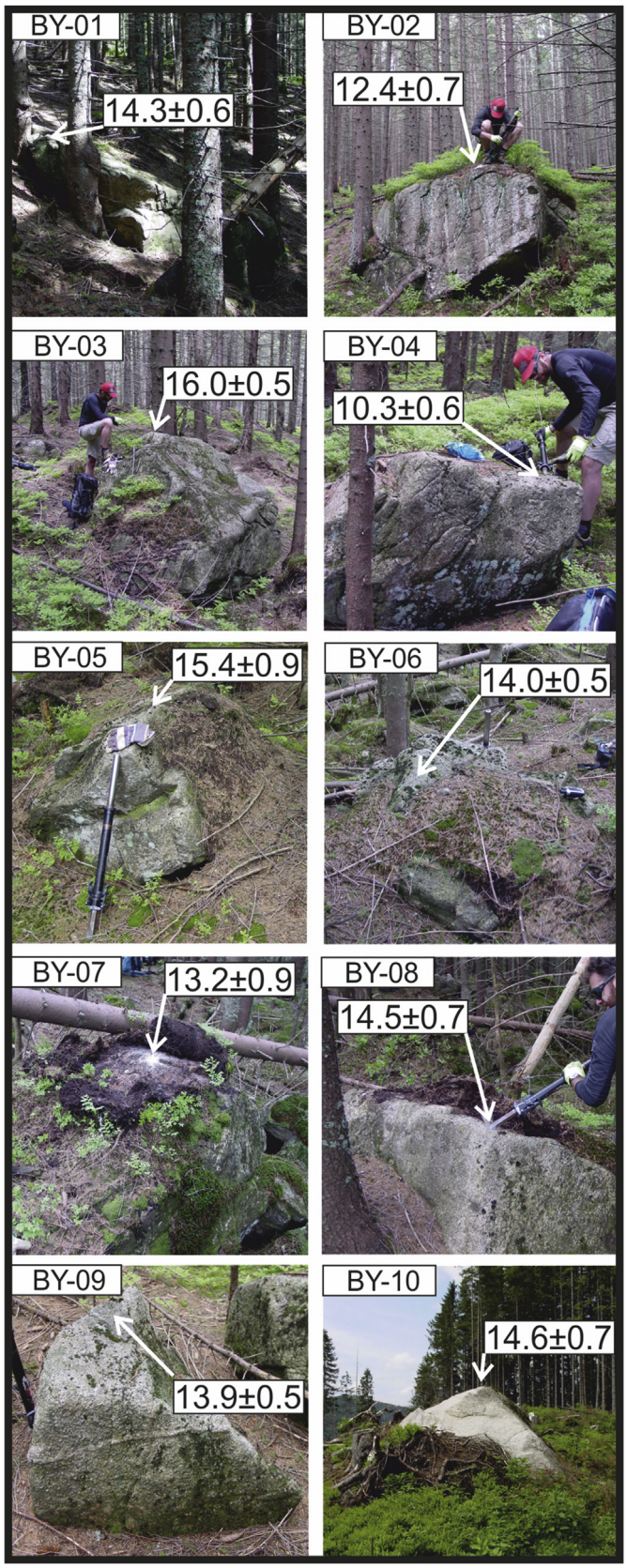

Fig. 5. Sampled boulders on the recessional moraine systems in the Sucha Kondracka (BY-01 to BY-05) and Sucha Kasprowa (BY-06to BY-10) valleys.

Technology (NIST) standard reference material 4325 using an assigned $^{10}Be/^{9}Be$ ratio of $(2.79 \pm 0.03) \times 10^{-11}$ (Nishiizumi et al., 2007) and a ^{10}Be half-life of $(1.36 \pm 0.07) \times 10^{6}$ years (Chmeleff et al., 2010; Korschinek et al., 2010). Analytical uncertainties (reported as 1 sigma) include a conservative 0.5% uncertainty based on long-term measurements of standards, a 1 sigma statistical error on counted ^{10}Be events, and the uncertainty associated with the chemical and analytical blank correction (the $^{10}Be/^{9}Be$ blank ratio was 20.88×10^{-15}).

3.1.3. Surface exposure age calculation

In order to determine surface exposure ages from the ^{10}Be concentrations measured in the quartz fractions, we used a modern global ^{10}Be production rate at sea level and high-latitude derived from a recalibrated global data set and recent calibration studies (Heyman, 2014) and the online version of the CRONUS-Earth calculator (Balco et al., 2009). A recently published Swedish ^{10}Beproduction rate (Stroeven et al., 2015) would generate slightly younger exposure ages.

We report here the exposure ages calculated with the “Lm” scaling schemes (Table 1). The “Lm” method provides the closest fit to existing calibration data and uses the scaling factors proposed by (Lal, 1991) and (Stone, 2000), and is further accommodated for paleomagnetic corrections following the description of Nishiizumi et al. (1989). As such, we think that the exposure ages calculated with this scaling method (Lm) represent the best age estimation of the exposure of the samples and we report in the result and discussion sections the exposure ages calculated with the global production rate and the “Lm” scaling method. The “Du” method is mainly a function of cutoff rigidity and atmospheric pressure (Dunai, 2001) and provides slightly older exposure ages. The “Li” method proposed by (Lifton et al., 2005) produces exposure ages slightly older than the “Lm” method and the “De” method proposed by (Desilets et al., 2006) produces exposure ages slightly younger than those calculated with the “Du” method. Using the recently developed LSD (Lifton-Sato-Dunai) scaling scheme by (Lifton et al., 2014) would increase our exposure ages by ~4%.

The CRONUS-Earth online calculator makes sample specific corrections for thickness and density (we assumed a density of 2.7 g cm^{-3}). The production rates could be affected by intermittent snow cover and erosion rate. We do apply a correction for snow cover as the valley receives substantial precipitation during the winter months. Samples between 1000 and 1199 m were corrected for 20 cm of snow for 90 days/year, samples between 1200 and 1599 m were corrected for 20 cm of snow for 120 days/year, and samples between 1600 and 2000 m were corrected for 20 cm of snow for 180 days/year. We also apply a 2 mm/ka erosion rate on our samples. This erosion rate is an estimate used to illustrate the possible effect of erosional processes on the exposure ages. A doubling of this estimate would increase the exposure age of a boulder exposed for 14.0 ka by <2% (~300 years). The production rates could be further affected by vegetation cover but we do not apply any correction for this factor as vegetation is mostly composed of young spruce trees. Finally, surface production rates were not corrected for sample surface slope as samples come from the top most flat surface of the boulders, but we do corrected the surface production rates for topographic shielding due to surrounding topography using the online topographic shielding calculator available at: http://hess.ess.washington.edu/math/. All exposure ages of moraine boulders were calculated with assumption of erosion and snow cover correction. All boulders were at least 1 m in diameter and strongly embedded within the matrix on the moraine's crests (Figs. 4 and 5). We interpret the results as minimum exposure ages.

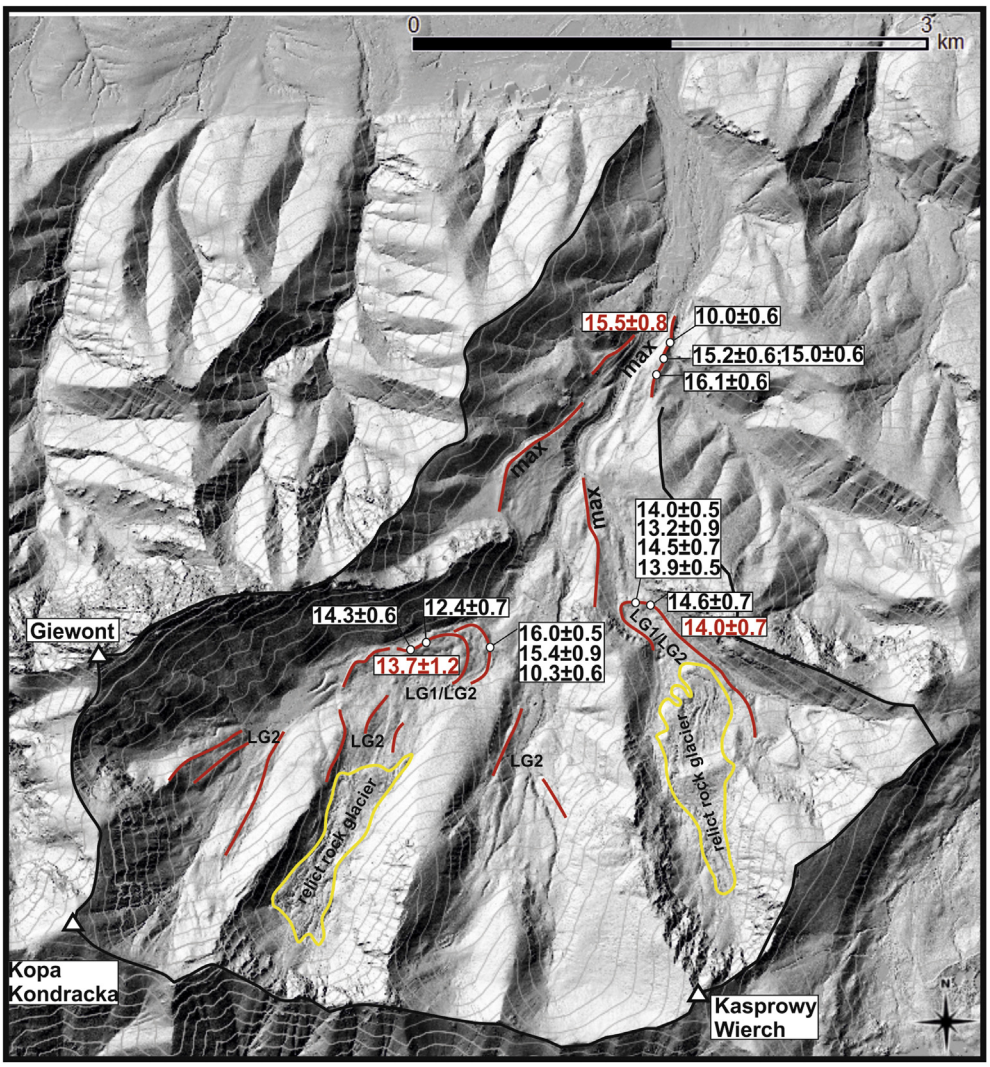

Fig. 6. Major terminal and lateral moraines (red lines) with exposure ages, fossil rock glaciers (yellow outline) and sample locations on the LIDAR digital elevation model of the study area. The mean ages of the moraines in red. The contour interval line (thin grey lines) is 50 m. (For interpretation of the references to colour in this figure legend, the reader is referred to the web version of this article.)

3.2. Glacier-climate modelling

In order to calculate the climatic parameters (mean annual temperature, mean summer temperature and annual precipitation) corresponding to steady state glacier terminus conditions we used two independent models which have been already used in the Tatra Mountains (Makos et al., 2013a and b).

3.2.1. Degree-day model

This model is a one dimensional ice flow model which reconstructs the glacier's profile along the valley axis and simulates horizontal and vertical extent of the active glacial ice (Sarikaya et al., 2008, 2009). The model simulates flow of ice induced by the annual mass balance of the glacier at any point along the topographic central flowline of the glacier. The mass balance is calculated as the difference between net accumulation and net ablation of snow. The elevation where mass balance equals zero represents the equilibrium line of the glacier.

Accumulation of snow is assumed when precipitation occurs below zero degrees. If air temperature is below or equal to 0 °C the whole precipitation supplies the glacial system with snow, above 0 °C it is rain. Total accumulation of snow is determined based on mean monthly temperatures and precipitation.

Ablation of snow and ice is calculated using the relation between the sum of positive air temperature and amount of melted snow and ice during the balance year. This relation is described as the positive degree-day factors which were used for the first time by Braithwaite (1995). In our study we applied relations calculated for alpine glaciers which are 3 mm day^{-1} °C^{-1} for snow and 8 mm day^{-1} °C^{-1} for ice (Braithwaite and Zhang, 2000). The modelled mass balance is used as the input for calculation of ice thickness and its growth using the equations of ice flow presented by Paterson (1994) and Haeberli (1996). While calculating the ice velocity, the model assumes only the ice deformation but no basal sliding. The basal shear stress, however, is calculated without contribution of the valley shape factor.

The modelling technique requires simulation of mean annual temperature and annual precipitation changes in relation to modern conditions. On that base model recreates the glacier along the valley axis accordingly to the mass balance determined by the temperature and precipitation. Particular scenarios with glacier existing in steady-state conditions occur while temperature

Table 1
^{10}Be sample characteristics and exposure ages from the Bystra catchment.

Sample ID	Lat N (DD)	Long E (DD)	Elevation (m a.s.l.)	Quartz (g)	Thickness (cm)[a]	Shielding factor[b]	Be carrier (10^{19} at)	[^{10}Be] (at g^{-1})[c]	^{10}Be age (ka) global PR[d]
Maximum moraine									**15.5 ± 0.8** [e]
BY-11	49.2653	19.9795	1107	15.9842	6.2	0.9933	2.0454	161597 ± 5552	16.1 ± 0.6
BY-12	49.2667	19.9804	1077	12.9424	5.4	0.9907	2.0404	149259 ± 5926	15.2 ± 0.6
BY-13	49.2667	19.9804	1077	11.4166	4.0	0.9907	2.0483	149226 ± 6183	15.0 ± 0.6
BY-14[f]	49.2674	19.9804	1057	9.72600	3.1	0.9907	2.0481	99325 ± 5631	10.0 ± 0.6
Sucha Kondracka V. LG1/LG2									**13.7 ± 1.2**[e]
BY-01	49.2500	19.9584	1302	13.2731	6.5	0.9808	2.0295	164971 ± 7261	14.3 ± 0.6
BY-02	49.2501	19.9611	1294	13.6900	4.7	0.9775	2.0365	144422 ± 7503	12.4 ± 0.7
BY-03	49.2503	19.9638	1292	12.7670	6.0	0.9860	2.0394	184823 ± 6001	16.0 ± 0.5
BY-04	49.2503	19.9638	1292	11.2742	4.5	0.9860	2.0446	122253 ± 6718	10.3 ± 0.6
BY-05	49.2503	19.9638	1292	7.82170	5.7	0.9860	2.0365	178935 ± 9592	15.4 ± 0.9
Sucha Kasprowa V. LG1/LG2									**14.0 ± 0.7**[e]
BY-06	49.2531	19.9772	1285	20.3054	4.2	0.9739	2.0505	161654 ± 5301	14.0 ± 0.5
BY-07	49.2531	19.9772	1285	10.3211	4.7	0.9739	2.0474	152599 ± 9658	13.2 ± 0.9
BY-08	49.2531	19.9772	1285	11.8675	3.6	0.9739	2.0382	168116 ± 7370	14.5 ± 0.7
BY-09	49.2531	19.9772	1285	22.0877	3.2	0.9739	2.0398	162471 ± 6072	13.9 ± 0.5
BY-10	49.2529	19.9779	1295	7.50210	3.2	0.9767	2.0416	171965 ± 7778	14.6 ± 0.7

[a] Sample tickness includes snow correction: samples between 1000 and 1199 m were corrected for 20 cm of snow for 90 days/year, samples between 1200 1599 m were corrected for 20 cm of snow for 120 days/year, and samples between 1600 and 2000 m were corrected for 20 cm of snow for 180 days/year.
[b] Azimuths and angular elevations (0–90°) to calculate the shielding factor were recorded using a compass and clinometer.
[c] All samples measured at the ASTER facility. AMS results are standardized to NIST_27900. ^{10}Be/^{9}Be ratios were corrected for a process blank value of 2.22 10^{-15}.
[d] All ages calculated using the developmental version of the CRONUS-Earth online 10Be exposure age calculator version 2.2 (http://hess.ess.washington.edu/math/al_be_v22/alt_cal/Heyman_compilation_input_aspublished.html) for the Global production rate (Heyman, 2014).
[e] Moraine age corresponds to the arithmetic mean and the error corresponds to the standard deviation of the mean. The error includes uncertainties associated to the measurement of the nuclide concentration, the scaling scheme (Lm), and the reference rate nuclide production. A standard atmosphere was used. An erosion of 2 mm/ka was used (see discussion in text). A rock density of 2.7 g cm^{-3} was used.
[f] Sample removed on the basis of Chauvenet's criterion. The sample was not used in the moraine age calculation.

decreases and precipitation changes from very wet conditions to extremely dry conditions. The modelling results are limited mainly by the length of the glacier but also by its thickness and mass balance. When the geometry of the glacier is simple with one accumulation area the glacier's length is the best limiting factor for the model. However, when there are several cirques or tributaries within the glacial system, the thickness of particular valley glaciers along the troughs is the main limiting factor. Moreover, in both cases the mass balance reconstructed by the model can be used. Usually, model output contains very wide range of scenarios from extremely dry and cold to extremely wet and warm conditions. Some of them are unrealistic for glacial systems in specific geographical location and when constrained by available proxy data. The required inputs for the ice-flow model are: the present-day topography of the valley, the spatial distribution of the present-day monthly mean temperatures, and the total precipitation along the glaciated valley. Valley topography was created from the digital elevation model of the study area (5 × 5 m). Long-term monthly mean temperature and precipitation data from meteorological stations (Zakopane, Kasprowy Wierch, Kalatówki, Myślenickie Turnie) located inside the massif and at the foreland were downloaded from the Global Historical Climatology Network and from the historical data provided by the Polish Institute of Meteorology and Water Management. All weather station data were transferred to sea level using the modern lapse rate, separately for each month. While modelling, the model recalculates temperature and precipitation values along the valley using the same lapse rates.

3.2.2. Ablation gradient model

This model was previously applied by Kull and Grosjean (2000) and Ivy-Ochs et al. (2006). The principle underlying this model is the reconstructed geometry of the glacier. This can be done if there is sufficient geomorphic records in the valleys and cirques. Two main features that limit glaciers extent are moraine ridges (terminal and lateral) and glacial trimlines. The terminal moraine determines the horizontal extent of the glacier, while lateral moraine marks the upper limit of the glacier tongue along the glacial trough. The glacial trimline is the boundary on the mountain peak or ridge below which there is evidence for glacial erosion such as striae or polish and above which the bedrock does not show such evidence, being jagged and frost-weathered. Typically, the trimline separates the steep and smooth part of the valley below and the jagged, shallower slope above (Ballantyne, 1997; Kelly et al. 2004; 2006; Brocklehurst et al. 2008). This means that the trimline approximates the former elevation of the active glacial erosion under the warm-based ice. Trimlines are observed within the trough walls as well as on the cirque walls. If the glacial forms are absent in some part of the slope then it is necessary to approximate the glacier's limit between existing forms, accordingly to the slope of the valley bottom with special attention for steps and overdeepenings.

Based on the glacier geometry, the principal parameters of the glacier can be measured: thickness, width, surface area, surface slope (Table 2), allowing to calculate the equilibrium line altitude (ELA) and the basal shear stress along the glacier. The ELA was calculated using the accumulation area ratio (AAR) determined on the basis of the relation by Kern and Laszlo (2010).

The basal shear stress is the crucial component for calculation of the total ice flow velocity (sliding and deformation). Both, the ice sliding velocity and deformation velocity have been determined using the sliding and deformation factors calculated by Budd et al. (1979). It follows that the ice-flux through the specified cross-sections can be calculated along the glacier's tongue between the ELA and the snout.

From the difference of ice flux between neighboring cross-sections and the surface area of the glacier between them, the net ablation of the surface increment can be estimated. The balance gradient ($\partial a/\partial z$) can be then calculated as the relation of the net ablation between neighboring cross-sections to the elevation of the glacier surface below the ELA. All necessary equations and variables are given in Ivy-Ochs et al. (2006)and Makos et al. (2013b). The ablation gradient is an input value to calculate annual precipitation and summer temperature.

For the palaeo-climatological interpretations we use the model

Table 2
Parameters of the Bystra glacier used for mass balance calculations. Cross-sections A-D refer to Fig. 12.

Cross-section	Width [m]	Thickness [m]	Surface slope [°]	Valley shape factor	Basal shear stress [kPa]
A	790	80	11	0.56	75
B	390	65	6	0.74	46
C	260	50	6	0.71	31
D	165	20	13	0.78	30

that was previously presented by Ivy-Ochs et al. (2006). The model calculates summer temperature (Ts) at the ELA as the parameter of ablation with annual precipitation (P) as the parameter of accumulation.

Ohmura et al. (1992) defined P as the sum of the winter accumulation and summer precipitation, and Ts as the free air temperature in summer (JJA) at the ELA. This relation is described as a regression equation:

$$P = 645 + 296Ts + 9Ts^2 \quad (1)$$

Based on the data set of Ohmura et al. (1992) and Kuhn (1984), Ivy-Ochs et al. (2006) suggested equations for calculating the summer temperature (Ts) and annual precipitation (P) at the ELA of the glacier. All equations are given in detail in Ivy-Ochs et al. (2006).

Results of both models can be compared mainly based on the sum of precipitation at the ELA as well as on the balance gradient at the glacier's front. Therefore, on that basis we can obtain the mean annual temperature and mean summer temperature, which are both controlled by precipitation.

4. Results

4.1. Deglacial chronology

We tested each moraine population for statistical outliers using Chauvenet's criterion (Taylor, 1997), a criterion identifying samples that have <50% probability of falling within the normal distribution of the sample population. Sample BY-14 was identified as an outlier and was removed from the moraine sample population before calculating the moraine age in Kuźnice (maximum moraine). For each moraine we report the arithmetic mean age and the associated uncertainties, which include the analytical uncertainties, the Lm scaling scheme uncertainty, and the production rate uncertainty (Table 1). Three samples from the maximum moraine were dated between 15.0 ± 0.6 and 16.1 ± 0.6 ka. The best estimate for the deposition time of the moraine is 15.5 ± 0.8 ka (Figs. 4 and 5). Five samples from the Kondratowa LG1/LG2 moraine were dated between 10.3 ± 0.6 ka and 16.0 ± 0.5 ka and the best estimate for the deposition time of the moraine is 13.7 ± 1.2 ka. Five samples from the Sucha Kasprowa LG1/LG2 moraine were dated between 13.2 ± 0.9 ka and 14.6 ± 0.7 ka and the best estimate for the deposition time of the moraine is 14.0 ± 0.7 ka (Figs. 5 and 6). The moraine ages from the Kondratowa LG1/LG2 and Sucha Kasprowa LG1/LG2 moraines are undistinguishable and most likely represent the same glacial event.

4.2. Glacier-climate modelling

We reconstructed the geometry of the glaciers existing in the Bystra catchment during the maximum advance and two recessional stages (LG1 and LG2) (Fig. 7–9). This reconstruction is based on the geomorphologic evidence, mainly on the position of terminal and lateral moraines as well as of glacial trimlines (Fig. 2).

Their position suggests that during the maximum advance within the accumulation area the active ice surface reached 1800 m a.s.l. on the cirques headwalls and declined slightly towards the confluence zone at 1300 m a.s.l. accordingly to the slope of the valley floor. The total area of the glacial system during the maximum extent was around 7.8 km^2. According to the relation by Kern and Laszlo (2010) its accumulation area ratio (AAR) was 0.62. This means that the equilibrium line altitude (ELA) of the glacier was located at the elevation of 1480 m a.s.l.

Post-maximum stabilization of glaciers occurred when the Sucha Kasprowa, Goryczkowa and Kondratowa glaciers became separate systems terminating at the elevation of 1250–1300 m a.s.l. The total area of the Sucha Kasprowa glacier during the first recessional stage (LG1) was 1.5 km^2. The AAR of this glacier is estimated to 0.51 and the ELA was located at 1530 m a.s.l. (Fig. 8) During the LG2 stage the Sucha Kasprowa glacier existed in a single basin and its former additional supplier remained isolated in the Stare Szałasiska Valley. The ELA of the glaciers in the Sucha Kasprowa Valley was located again at 1530 m a.s.l. during the LG2 stage (Fig. 9).

The total area of the Kondratowa glacier was 2.5 km^2 and the AAR of the glacier is calculated to be 0.54. The ELA was located at the elevation of 1520 m a.s.l. during the first recessional stage (Fig. 8). Then the glacier broke up and at the subsequent LG2 stage there were two separate glaciers: Sucha Kondracka glacier and Kondratowa glacier. Their ELA remained at the same position as during the LG1 stage (Fig. 9).

Despite the absence of terminal or lateral moraine in the Goryczkowa Valley we reconstructed the geometry of the glacier assuming its snout position at the elevation of around 1250 m a.s.l. where the glacial relief remains hummocky moraine. The elevation of the glaciers front is consistent with the two adjacent valleys. Our reconstruction indicates the total area of the Goryczkowy glacier of 1.3 km^2. Its AAR was then 0.50 and ELA was located at 1600 m a.s.l. (Figs. 8 and 9).

The Bystra glacier during the maximum advance in the catchment could have reached the reconstructed geometry while temperature decreased by 8–14 °C and precipitation changed between +80% and −80%, respectively in relation to present-day conditions (Fig. 10). The range of reconstructed climatic conditions is controlled by the ice thickness along the accumulation area which during the maximum advance was located within three main tributaries (Kondratowa, Goryczkowa and Sucha Kasprowa valleys).

Modelling results for Kondratowa, Goryczkowa and Sucha Kasprowa glaciers existing during the first recessional stage are almost identical and were obtained using the glacier's length (2300, 2250 and 2260 m, respectively) as the limiting factor. All three glaciers existed in steady state conditions when temperature was lower than today by 7–13 °C and annual precipitation was doubled or lowered by 80%, respectively (Fig. 10). These wide-ranged climatic parameters determined the ELA position between 1340 and 1500 m a.s.l. and ablation gradients along glacier's tongue between 0 mm/100 m and 650 mm/100 m. All scenarios in which the ablations gradient drops almost to zero are considered to be unrealistic.

In addition, because the degree-day model for the maximum Bystra glacier was limited mainly by the thickness of particular

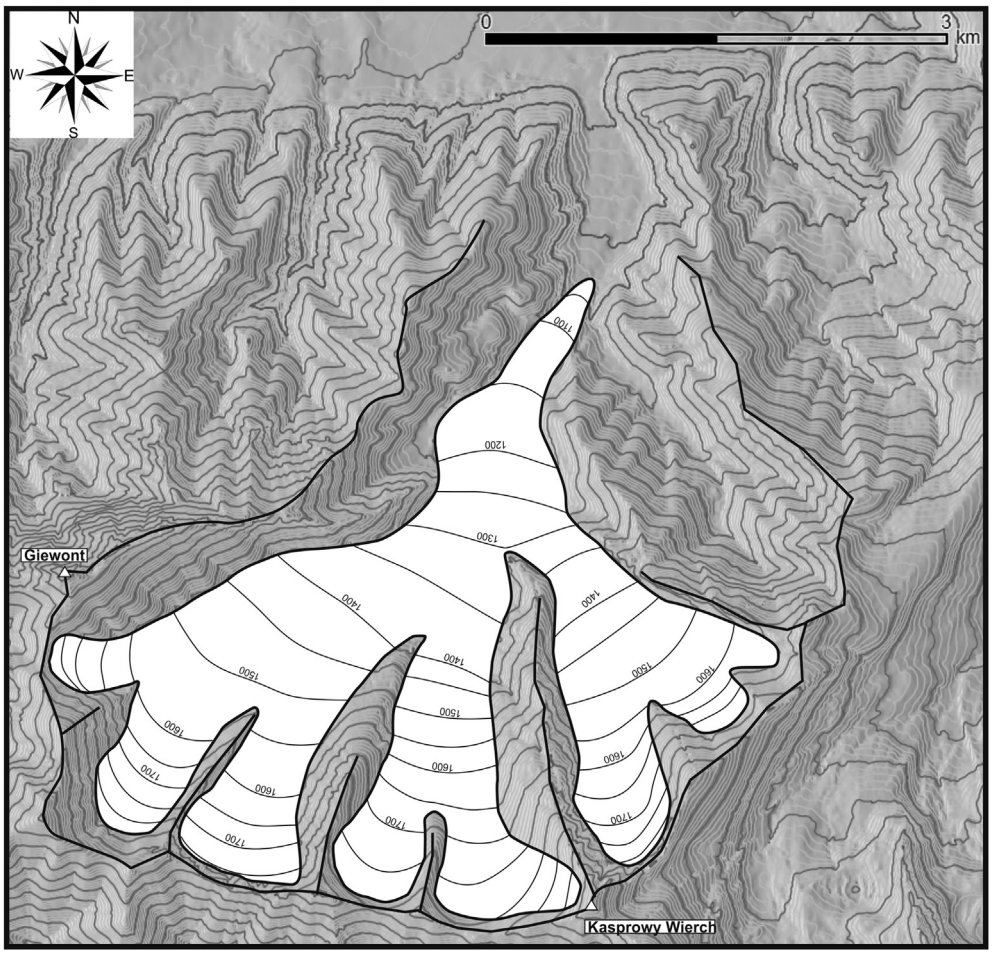

Fig. 7. Reconstructed geometry of the Bystra glacier during the maximum advance. The contour interval is 50 m.

tributaries, we decided to apply the ablation gradient model to reconstruct the ablation gradient along the glacier below the ELA and on that basis calculate summer temperature and annual precipitation at the ELA following the relation by Ohmura et al. (1992) and Ivy-Ochs et al. (2006). We assumed six scenarios of sliding contribution in ice velocity between 70 and 95% (Table 3). For such scenarios the ablation gradient of the Bystra glacier could have reached values from 98 mm/100 m to 550 mm/100 m. The summer temperature at the ELA oscillates between −3.6 and 2 °C and annual precipitation is from 40 to 1360 mm.

5. Discussion

5.1. Timing of moraine formation

When considering the moraine exposure ages it should be emphasized that the cold climatic pulse responsible for glacier advance or stillstand must have occurred at least few tens and more likely few hundred years earlier, due to the glacier reaction time to full glacial conditions (e.g. Ivy-Ochs et al., 2006). This reaction time is controlled mainly by the size of the glacier, the temperature and precipitation that determine its mass balance and by consequence the velocity of ice movement. Warmer and wetter conditions usually cause higher balance gradients along the glacier and thus higher velocity of ice movement that decreases the reaction time. Therefore, during the gradual deglaciation, the particular stages when glacier remained in steady-state conditions should have shorter reaction times.

According to the position of the maximum moraine, its age is surprisingly young. Other maximum moraines in the High Tatra Mountains that have been dated so far using the ^{36}Cl dating method, indicate the age of their formation during the global LGM (26.5–19 ka – Clark et al., 2009) between 25 and 21 ka (Makos et al., 2014; Makos, 2015) (Fig. 11). While ^{36}Cl and ^{10}Be ages may not be directly comparable (Wilson et al., 2013), the maximum moraine in the Bystra catchment represents an unusual case compare to other mountain ranges across Europe, where most of maximum moraines were formed during the global LGM (e.g. Engel et al., 2014; Ivy-Ochs, 2015; Delmas, 2015; Ruszkiczay-Rüdiger, in press). The mean age of the maximum moraine in the Bystra Valley suggests the most extensive advance of the glacier during the LG. Final stabilization of the moraine at 15.5 ka may indicate that this advance was determined by the climate cooling during the Greenland Stadial 2.1a (OD) (Rasmussen et al., 2014) (Fig. 11). If the age of moraine is correct, we can consider at least four scenarios, explaining the absence of the LGM moraine in the catchment.

First, the LGM glacier was terminating at a position behind the maximum moraine up-valley in the Bystra catchment and therefore, during the LG advance the older moraines were overridden and destroyed.

Second, the LG glacier reached the same or a very similar position to that of the LGM and the LGM moraine system was rebuilt and rejuvenated significantly. However, in such case we should expect evidence of accretion within the maximum moraine or at

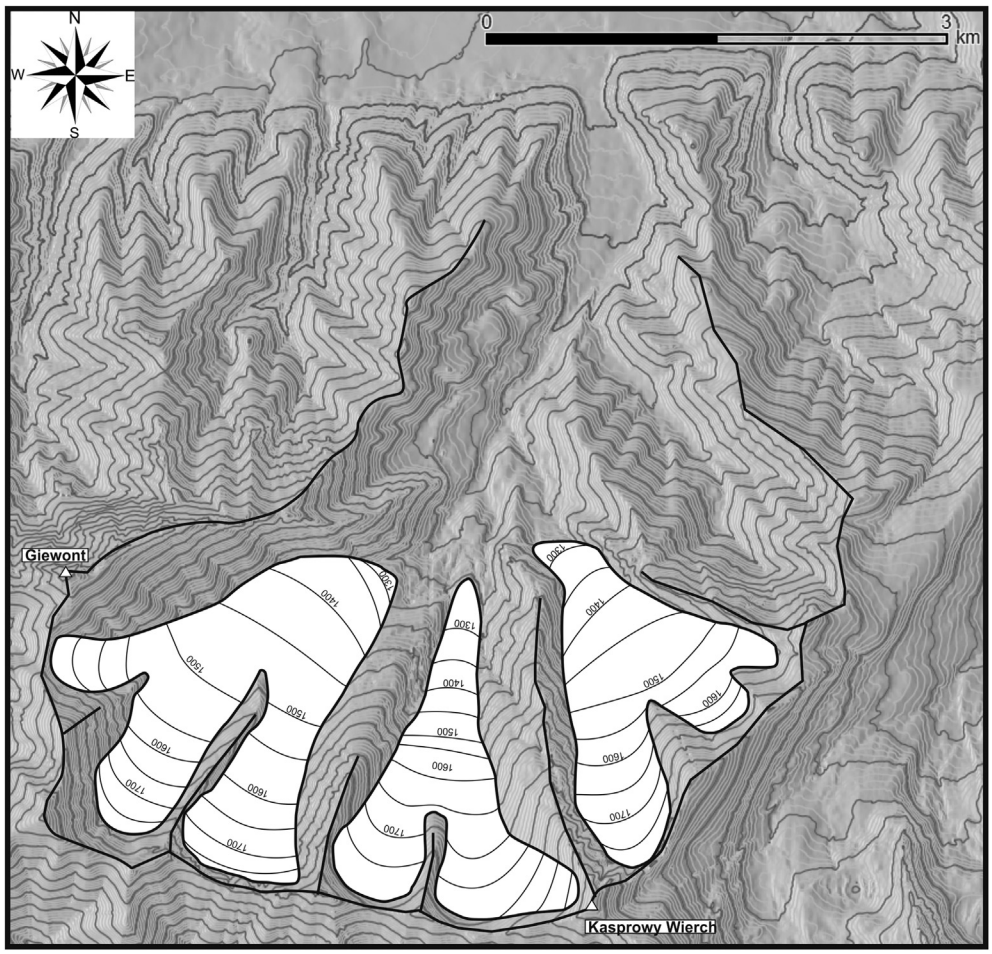

Fig. 8. Reconstructed geometry of the Sucha Kasprowa, Gorzyczkowa and Sucha Kondracka glaciers during the first recessional stage LG1. The contour interval is 50 m.

least multi-crested moraine system as it is observed in valleys where older moraines were cut by younger oscillations (e.g. Sarikaya et al., 2014). Moreover, in the High Tatra Mountains, the horizontal extent of the first LG advance was a few kilometers shorter than the LGM one (Makos et al., 2013a, 2014). In consequence, this would document significant discrepancies between ELA positions in the High Tatra Mountains and in the Bystra catchment. In the Biała Woda catchment the LG ELA was located at 1650 m a.s.l. (Makos et al., 2013a), therefore if the maximum advance in the Bystra catchment took place during the LG, then the ELA position of the Bystra glacier (1480 m a.s.l.) would be almost 170 m below that in the High Tatras. However, the LGM ELA in the adjacent Sucha Woda catchment and further east in the Biała Woda catchment was located at 1460 m a.s.l. in strong agreement with the one reconstructed for the Bystra glacier (Makos and Nitychoruk, 2011; Makos et al., 2014). If indeed the Bystra glacier maximum advance occurred during the LG, significant implications for palaeoclimatic conditions should be anticipated in the Bystra catchment at that time. We further discuss these implications in section 5.2.

The third scenario assumes that the LGM glacier was more extensive than the LG one but the moraine is no longer preserved in the valley. This would require unusual conditions at the front of the glacier not favorable for classic processes of moraine formation. This might be a calving glacier front terminating in a lake. This is an unprecedented situation in the Tatra Mountains and also very doubtful in the Bystra catchment, because there were no lake sediments recorded in the valley or in the foreland of the Tatras (e.g. Klimaszewski, 1988 and references therein).

Finally, it needs to be clearly stated that the exposure ages of boulders may reflect different exposure histories. Deposition of boulders at the front of the stagnant glacier is the major activity that is considered while studying the deglaciation of the mountain valleys. However, a number of post-depositional processes are also very important and they may have crucial significance for exposure histories of moraine boulders and therefore for chronological interpretation. Such scenario seems to be reasonable in the case of the maximum moraine in the Bystra Valley. The relatively sharp-crested ridge is located between two valleys (Bystra and Jaworzynki) that are drained by rivers cutting the 400 m long moraine directly at the foot of the moraine and this from both sides (Fig. 4). According to the model of Putkonen et al. (2003, 2008), the crest of a moraine ridge is very sharp and composed of numerous boulders shortly after deposition. This ridge remains under the influence of erosion and its cross-profile changes through time reflecting rounding and lowering of the crest and relocation of the large boulders from the top to the sides. We interpret the exposure ages of the four boulders to indicate post-depositional degradation of the moraine crest likely induced by fluvial sapping of the moraine base (Fig. 4). Moreover, the moraine ridge also decreases from S to N between 1110 and 1020 m a.s.l. and the boulders that are present on the crest could have been removed from their original position by solifluction and rolling probably during the LG when the relatively fresh moraine was eroded by meltwater from glaciers in the upper

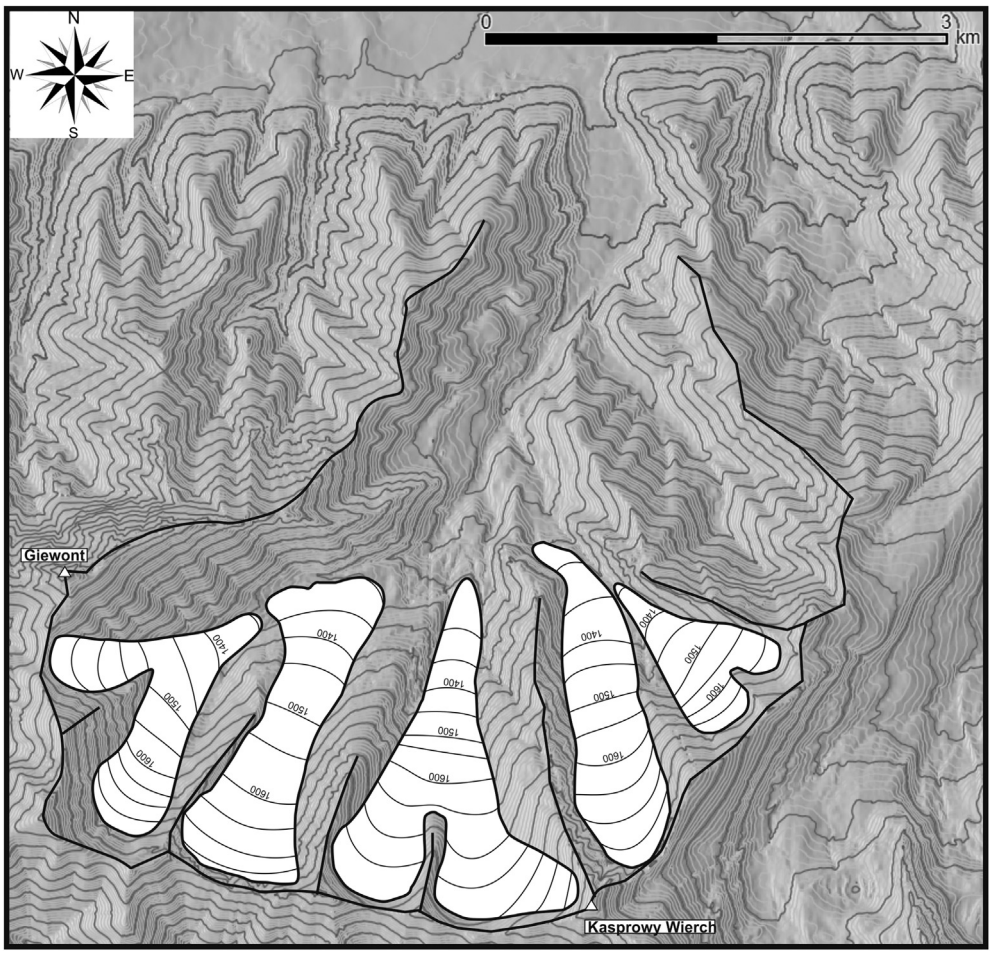

Fig. 9. Reconstructed geometry of the Stare Szałasiska, Sucha Kasprowa, Gorzyczkowa, Sucha Kondracka and Kondratowa glaciers during the second recessional stage LG2. The contour interval is 50 m.

part of the Bystra catchment. Therefore, the relatively young exposure ages reported from the maximum moraine in the Bystra Valley may not reflect the time of moraine deposition but could rather reflect post-depositional erosional processes that determined the current shape of the ridge. Moreover, the spatial distribution of ages along the ridge suggests that the lowermost part of the moraine indicates the strongest influence of erosion by the two converging rivers directly to the north of the ridge. The youngest exposure age (10.0 ka) is found at the lowest elevation compared the exposure ages obtained from the upper part of the ridge that could have stabilized as early as 16.1 ka. The altitude/age gradient could confirm the strongest fluvial erosion in the lowermost part of the ridge. This seems to be reasonable in the context of the moraine position with respect to the confluence zone of both erosive rivers.

Considering all the above scenarios two different chronology interpretations could be presented for the maximum advance in the Bystra Valley. If the moraine age reflects the timing of its deposition then this ridge would have been produced during the cooling of the Greenland Stadial 2.1a (OD) and the LGM moraine is absent within the catchment. If the moraine was eroded after deposition, however, and the exposure ages reflect activity of post-depositional processes, the ridge would have been formed likely during the LGM as other dated maximum moraines in the Tatra Mountains (Fig. 11). The latter chronology seems much more likely when compared to the other mountain ranges in Europe e.g. Alps (Ivy-Ochs et al., 2008; Ivy-Ochs, 2015), Pyrenees (Pallàs et al., 2006; Delamas et al., 2011; Delmas, 2015), Balkans (Kuhlemann et al., 2008, 2013) and Southern Carpathians (Ruszkiczay-Rüdiger, in press).

Two recessional moraine systems in the Kondratowa and Sucha Kasprowa valleys gave mean ages of 13.7 ± 1.2 ka and 14.0 ± 0.7 ka, respectively.

The terminal moraine in the Kondratowa Valley is a part of a composed moraine system which contains at least two ridges (the outer and inner ones). The geomorphology of this moraine system suggests more complicated pattern of deglaciation in the area. The NE part of the moraine indicates the maximum position of the glacier (LG1), however, the ridges located further inside the valley were likely produced during the younger oscillation (LG2). If the mean age of the form reflects its final stabilization during the LG2 oscillation, the climatic impulse could have occurred few hundred years earlier. According to the Greenland Ice Core chronology this might be during the Late-glacial Interstadial 1 (Bølling/Allerød Interstadial) when a cold event took place at around 14 ka (GI-1d – Older Dryas) (Fig. 11). Therefore, the LG1 advance occurred before Bølling warm period, during the Oldest Dryas (Greenland Stadial 2.1a) but the exact timing of this stage in the Bystra catchment is not known. Based on the geomorphologic evidence we were able to reconstruct the geometry of glaciers during both the LG1 and LG2 stages. The distribution of moraine ridges in the lowermost section of the ablation area of the LG1/LG2 glaciers suggest that despite the similar horizontal extent of both stages the LG1 and LG2 glaciers

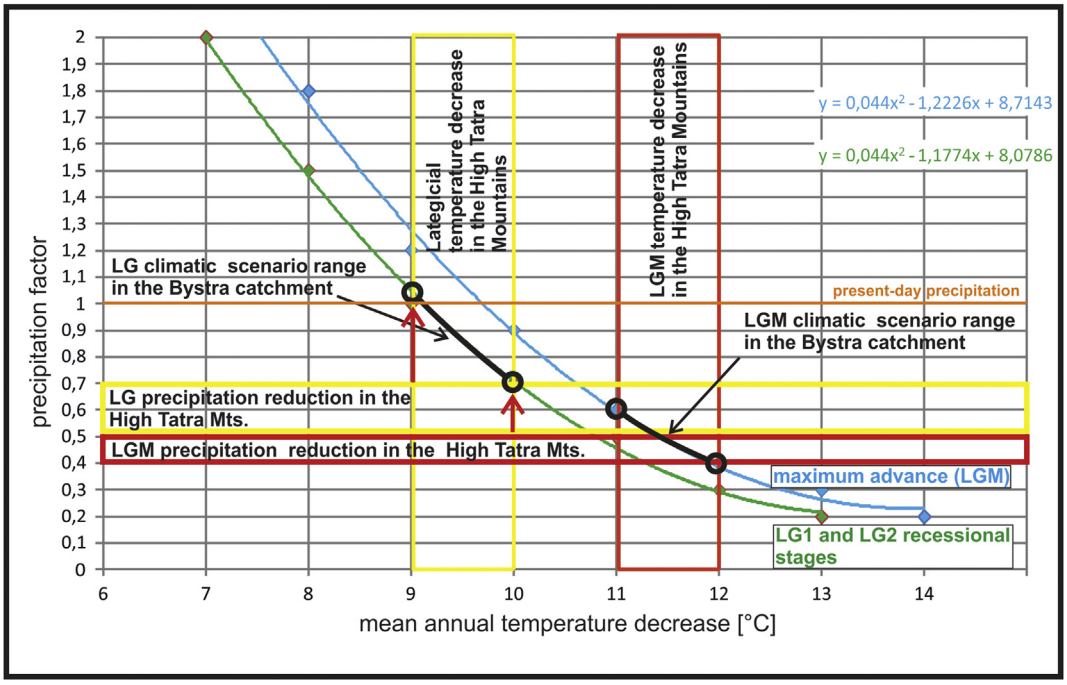

Fig. 10. Plot of glacier-climate modelling results in the Bystra catchment. Blue and green lines represent the range of climatic scenario when glaciers reached the position of moraines from LGM and LG1, respectively. Range of climatic parameters reconstructed for the LGM and Lateglacial (in red and yellow, respectively) in the High Tatra Mountains based on Makos et al. (2013a and 2014). Black lines with circles represent the most likely scenarios for Bystra catchment. They are limited based on the data set from the High Tatras as well as other proxy data from Central Europe and the Carpathians (Allen et al., 2008; Feurdean et al., 2008; Strandberg et al., 2011; Heyman et al., 2013; Ruszkiczay-Rüdiger et al., in press). Red arrows show the potentially 20–30% higher precipitation in the study area than in the eastern part of the massif during the Late-glacial. (For interpretation of the references to colour in this figure legend, the reader is referred to the web version of this article.)

Table 3
Palaeoglaciologic and palaeoclimatic characteristics of the LGM in the Bystra catchment.

Sliding contribution	70%	75%	80%	85%	90%	95%
Ablation gradient [kg/m^2/m]	−0.98	−1.70	−2.18	−2.93	−4.40	−5.55
Precipitation [ELA] [mm]	39	287	443	675	1086	1361
Temperature June - August [ELA] [°C]	−3.57	−1.62	−0.88	0.015	1,28	1.99
ΔT JJA [°C]	**−14**	**−12**	**−11**	**−10**	**−9**	**−8**
ΔP annual [%]	**−97**	**−80**	**−70**	**−55**	**−30**	**−10**

had significantly different geometry, especially in the ablation area (Fig. 2, 8 and 9). During the post-LG1 deglaciation (Bølling Interstadial), the Kondratowa glacier was losing mass along the southern slope of Giewont where solar radiation (higher temperature) effectively increased the rate of ablation. Therefore, the Sucha Kondracka and Kondratowa glaciers lost contact between themselves and during the subsequent LG2 oscillation both glaciers remained separated.

The termino-lateral moraine in the Sucha Kasprowa Valley was sampled at its northernmost part and all exposure ages are nearly concordant providing ages between 13.2 ± 0.9 ka and 14.6 ± 0.7 ka with a mean moraine age of 14.0 ± 0.7 ka (Fig. 6). Therefore, the termino-lateral moraine in the Sucha Kasprowa Valley reflects glacial activity during the LG2 stage. The lateral ridge is separated from the valley wall by a deep erosional cut which was most likely a marginal channel for melt water during the deglaciation of the area. This moraine was accumulated when the snout of the glacier melted-down strongly, especially along the southern slope of the Zawrat Kasprowy. It seems that the solar radiation was the main factor inducing the increased ablation rate also here. The position of the left arm of the terminal moraine shows that the vertical extent of the glacier on the right side of the valley was at least 30 m higher than the present-day position of the right lateral ridge. This may suggest formation of the moraine system during two stages. The position and exposure age of the right side moraine reflect the LG2 cold stage at around 14 ka, however, the left side moraine limits the glacier extent during the previous stage (LG1). The LG1 glacier was composed of two valley glaciers: the Sucha Kasprowa glacier and the Stare Szałasiska glacier. During the subsequent Bølling warming the snout of the Stare Szałasiska glacier retreated up-valley. During the LG2 stage the Sucha Kasprowa glacier reached the position of LG1 moraine again, accumulating a long arm of the lateral moraine located along the southern slope of the Zawrat Kasprowy. This episode occurred likely during the short cooling of the GI-1d at around 14 ka and the LG1 stage occurred likely during the pre-Bølling cold stage (Oldest Dryas) (Fig. 11).

The LG2 stage in the Bystra catchment correlates well with the GI-1d climate oscillation (Older Dryas). This is the first chronological evidence of a glacial cold stage at 14 ka in the Tatra Mountains. It seems that the glacier stillstand during the LG2 stage occurred simultaneously with the M3 advance in the Retezat Mountains (Ruszkiczay-Rüdiger et al., in press).

The extensive debris covers in the Sucha Kondracka and the Sucha Kasprowa valleys indicate a mass movement activity likely during the B/A Interstadial, of which oscillating climatic conditions favored instability of cirque walls. The large number of gullies

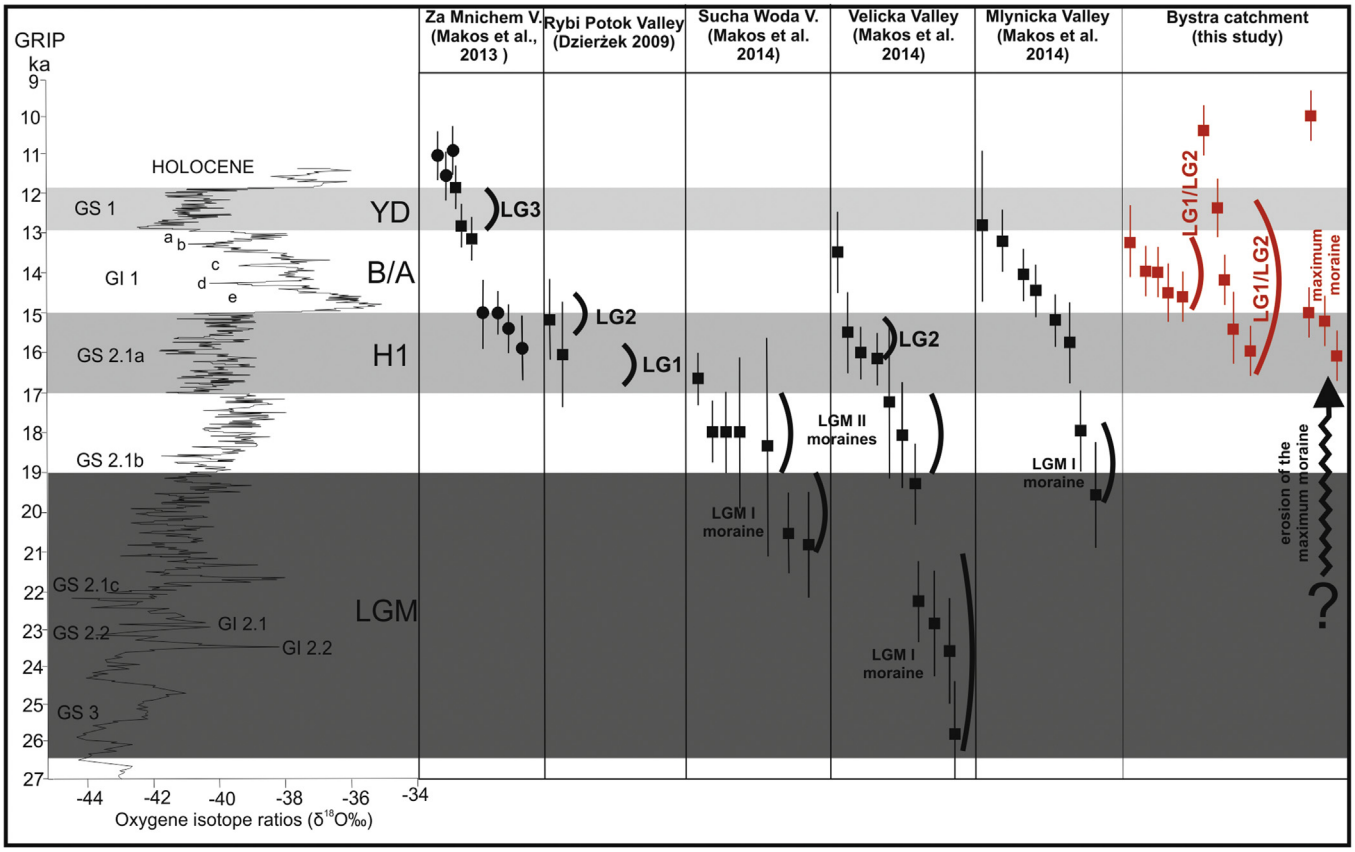

Fig. 11. Plot of exposure ages for samples from the study area and other locations in the Tatra Mountains against the GRIP ice-core record (Rasmussen et al., 2014). Shaded bands correspond to published time ranges of the LGM (Clark et al., 2009), the H1 event (Hemming, 2004), the Bølling/Allerød and the YoungerDryas (Rasmussen et al., 2014). Squares show samples from the moraine boulders and circles those of samples from the bedrock surfaces below glacial trimlines.

among these walls as well as the abundance of rock-fall cover below, record that a huge volume of rocks was transported from the slopes into the valley axis, probably directly onto the surface of melting glaciers. The morphology of the debris covers with numerous lobated and elongated ridges suggests that they were reworked by periglacial activity and existed as a rock glaciers during the LG and maybe even until the onset of Holocene.

The chronology from the Bystra catchment indicates three episodes of glacial activity. The oldest one occurred probably during the LGM, however, exposure ages do not reflect such timing due most likely to post-depositional erosion of the maximum moraine in Kuźnice. The first recessional stage LG1 is inferred based on geomorphologic record and it occurred probably during the pre-Bølling cold stage (Oldest Dryas) when the Kondratowa and Sucha Kasprowa glaciers terminated at the elevation of 1250 m a.s.l. for the first time (Figs. 8 and 11). Subsequent glacier stillstand at around 14 ka (GI-1d) allowed formation of terminal and lateral moraines of LG2 stage. The Sucha Kondracka and Sucha Kasprowa glaciers reached the elevation of 1250 m a.s.l. again, however, their former tributaries terminated separately higher up-valleys at that time (Figs. 9 and 11).

5.2. Palaeoclimatic interpretation

Both model used for this reconstruction gave a very wide range of results that need to be considered in the light of proxy data (palaeobotanical studies, ocean-atmosphere models), which can significantly restrict the calculated values.

The maximum advance of the Bystra glacier, based on evidence presented above, is assumed to have occurred during the global LGM. If so, the degree-day model indicates 8–14 °C lower temperatures and −80% to +80% change of precipitation during that time. These results were modelled for the three main tributaries (Kondratowa, Goryczkowa and Sucha Kasprowa glaciers) of the Bystra glacier. These tributaries had glaciers with ice thicknesses, of 70 m, 100 m and 90 m, respectively. In case of a compound glacial basin this is the only possible limiting factor when using the one-dimensional ice-flow model. However, these results are in the range of reconstructed LGM climatic parameters in the High Tatra Mountains (Makos et al., 2014). They were restricted based on ice thickness, ELA position as well as ablation gradient of the Velicka and Mlynicka glaciers. In addition, temperature data were compared to the modelling results with central European palaeoclimate proxies reported by Jost et al. (2005), Kageyama et al. (2006), Allen et al. (2008); Heyman et al. (2013) and Strandberg et al. (2011). These proxy data indicate that the LGM temperature decrease in relation to modern conditions at the level of 11–12 °C (Fig. 10). Such cooling requires 50–60% drier conditions in the High Tatras (Makos et al., 2014) and 40–60% lower precipitation in the Bystra catchment to preserve glaciers in stable conditions (Fig. 10). Thus, the LGM climatic conditions in the High Tatras and in the Bystra catchment are comparable and are supported by the almost identical position of the ELA (1460 m a.s.l.) and can be considered as reasonable parameters controlling the mass balance of glaciers during that time.

The ablation gradient model applied for the ablation area of the Bystra glacier gave also a wide range of possible conditions for stable glaciers (Fig. 12; Table 3). The diversity between particular

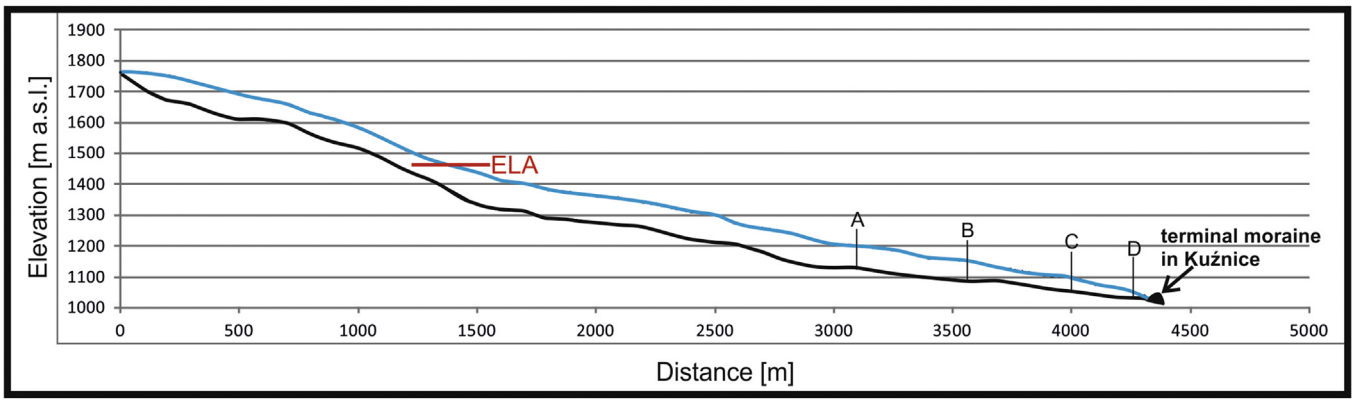

Fig. 12. Longitudinal profile of the Bystra glacier during the maximum advance. Cross-sections A, B, C and D were used for calculation of mass balance and ablation gradient along the glacier's tongue between cross-section A and terminal moraine. Detailed methodology of calculation in Ivy-Ochs et al. (2006). Details for calculation in Table 2.

scenarios is controlled mainly by the sliding contribution in the total velocity of the glacier which is assumed to reside between 70% and 95%. Such values are reasonable for warm-based glacier, which is drained by a well-developed subglacial system, although we do not know the exact thermal regime of the Bystra glacier. Assumption on its hydrologic regime can be made based on the glacial morphology of the valley, which shows effective subglacial erosion with a significant contribution of pressurized water flow, as shown by valley topography. According to the study by Gądek (1998), a glacier of average thickness of ~50 m has a relation between basal sliding and the total velocity above 0.5, typically between 0.8 and 0.975. These values correspond to the velocity values found for the Bystra glacier. These values determine the ablation gradient along the tongue between 97 mm 100 m^{-1} (70% sliding) and 545 mm 100 m^{-1} (95% sliding). The former scenario is extremely cold and dry, however the latter one is much warmer and wetter. If the basal sliding is only 70% of the total velocity, the annual precipitation sum at the ELA of the glacier (1460 m a.s.l.) will be around 40 mm and the mean summer temperature (JJA) will reach −3.6 °C. On the opposite side, the 95% sliding gives the precipitation at the level of 1360 mm and the T (JJA) of 2 °C. The present-day precipitation and mean summer temperature at the level of the LGM ELA are 1500 mm and 10.3 °C, respectively. Thus, according to the ablation gradient model and the assumed scenarios, the LGM annual precipitation was lower than today between 97% and 10% and T (JJA) decrease was between 14 °C and 8 °C, respectively. These two radical scenarios reflect rather extremely dry and wet conditions according to the proxy data from central Europe (Jost et al., 2005; Kageyama et al., 2006; Allen et al., 2008; Heyman et al., 2013; Strandberg et al., 2011) and some scenario in between will be more plausible. Our data set suggests that aa 85% sliding scenario gives the most reasonable climatic parameters for the LGM Bystra glacier. The ablation gradient of the glacier is then ~300 mm 100 m^{-1}. Such mass balance was controlled by the precipitation and T(JJA) at the ELA of 670 mm and 0 °C, respectively. This means colder and drier conditions than present-day ones by about 10 °C and 55%. This is in accordance with the reconstructions made in the High Tatra Mountains where Sucha Woda and Biała Woda glaciers have been modelled (Makos and Nitychoruk, 2011; Makos et al., 2014). Such scenario is also in agreement with results of the degree-day model where 11–12 °C mean annual temperature reduction gave precipitation decrease of 50–60% in relation to the modern values. In summary, our modelling results show that the Bystra glacier during the LGM was a warm-based glacier with sliding contribution of ~85% and is in general agreement with glaciological assumptions for valley glaciers of that size (Gądek, 1998).

We also considered the scenario when the maximum advance in the Bystra catchment occurred during the LG. The former palaeoclimatological studies in the High Tatra Mountains (Makos et al., 2013a) indicate a LG mean annual temperature decrease of around 9–10 °C. This gives 30–50% lower precipitation than today. The modelling results for the Bystra glacier suggest a significantly different situation. If the temperature drop reached 9–10 °C then the precipitation would have been from +30% to −10%, respectively (Fig. 10). Therefore, the same temperature scenario for the High Tatras and the Bystra catchment requires much more moisture (up to 60%) in the study area and even wetter (+30%) conditions than today. Available palaeobotanical data from the Tatra's foreland, however, indicate a tundra-like vegetation and rather cold and dry conditions during the GS2.1a (OD) (Koperowa, 1962). Much drier conditions (40–50%) than today were also inferred in Central Carpathians (Feurdean et al., 2008). Moreover, the ablation gradient model of the Bystra glacier indicates that mean summer temperature decrease of around 8 °C during the GS2.1a (Renssen and Isarin, 2001) would require only a slight (10%) reduction in precipitation. There is thus a significant discrepancy in precipitation scenarios between the study area and the High Tatras as well as the Central Carpathians when we assume that the maximum advance of the Bystra glacier took place during the OD. An LGM age for the maximum advance is the more likely scenario for the Bystra catchment and is supported by the Late Pleistocene glacial chronology in the High Tatra Mountains as well as the results of glacier-climate modelling.

The recessional stages LG1 and LG2 both occurred during the Lateglacial and are correlated with the GS-2.1a (pre- Bølling) and GI-1d (Older Dryas), respectively. The glacier-climate modelling for both stages was done using the degree-day model. The horizontal distance between moraines of both stages as well as the pattern of deglaciation described in detail above do not allow for two separate simulations due to the limited resolution of the one-dimensional ice flow model. The close position of the glacier fronts during the LG1 and LG2 stages suggests that they were both controlled by very similar climatic conditions. Modelling results show that the existence of all three LG glaciers in the Bystra catchment (Kondratowa, Goryczkowa and Sucha Kasprowa glaciers) was determined by the same conditions with mean annual temperature decrease of 7–13 °C and precipitation change between +100% and −80%, respectively (Fig. 10). This wide range of scenarios needs to be constrained with available proxy data. The temperature record in the Central Carpathians during the OD indicates lower values than today by ~7 °C (Feurdean et al., 2008). Renssen and Isarin (2001), however, suggest a GS-2a annual temperature decreased of ~12 °C

in southern Poland. In the central Alps, the mean summer temperature was lower than today by 8.5–10 °C and precipitation was only 30% of today's values (Ivy-Ochs et al., 2006). In the High Tatra Mountains, however, the most reasonable temperature reduction during the GS-2.1a was in the range of 9–10 °C and the precipitation was reduced by 30–50% compared to modern values (Makos et al., 2013a; Makos, 2015) (Fig. 10). Such cooling in the Bystra catchment requires higher precipitation than in the High Tatras. Our modelling results show that if the temperature decrease was 9 °C, the precipitation must have been about the same as today. However, 10 °C cooling determines 30% lower precipitation. Half of today's precipitation in the Bystra Valley could have occurred when temperature was 11 °C lower than today (Fig. 10). For every temperature scenario the precipitation in the study area is between 20% and 30% higher than in the High Tatra Mountains. But the relatively small area of the Tatra Mountains and in consequence the small distance between particular catchments suggests a rather uniform horizontal distribution of temperature. Therefore, we assume a constant temperature decrease along the northern fringe of the massif during the LG. Our results indicate that the glaciers in the western part of the massif were supplied with more moisture during the LG. All cirque floors in the Bystra catchment and LG ELA's are located approximately 100–150 m lower than in the High Tatras and the glacier's fronts in both the Western and High Tatras reached almost the same elevation of 1250–1300 m a.s.l. Therefore, the precipitation and general moisture supply in the Bystra catchment were likely higher than in the eastern part of the massif and influenced the relatively long extent of the glaciers. The higher precipitation in the Western Tatra Mountains could have been controlled by the atmospheric circulation pattern over central Europe during the LG with the main moisture transport coming from the west and north-west. The prevailing NW wind direction during cold phases of the Pleistocene was suggested based on the spatial distribution of cirques in the High Tatra Mountains (Křížek and Mida, 2013). Thus, slightly higher amount of precipitation was probably received in the western catchments. Such diversity is observed also currently, where two third of the year is controlled by the air masses inflow from the NW (Niedźwiedź, 1992). There is about 10% more precipitation falling in the Western Tatra Mountains (Ornak meteo station - 1480 mm) than in the High Tatra Mountains (Roztoka meteo station - 1350 mm), when measured at the same elevation of 1050 m a.s.l. The additional factor that may have determined higher amount of accumulation was a relatively smooth relief of the main mountain ridges around the Bystra catchment with deep and wide cols that served as corridors for wind-blown snow from adjacent valleys and cirques. According to the proxy data from the northern Tara's foreland (Koperowa, 1962) a scenario of 9 °C cooling with the present-day amount of precipitation during the GS-2.1a seems unlikely and we suggest that a scenario with 30% drier conditions and 10 °C colder temperature than today to be more likely.

6. Conclusions

The glacial geomorphologic imprints in the Bystra catchment coupled with the exposure age chronology based on ^{10}Be dating indicate that Late Pleistocene glaciation took place in the study area: the maximum advance at the elevation of 1020 m a.s.l. and two recessional stages, of which terminal moraines are preserved between 1250 and 1350 m a.s.l. Despite the LG exposure age of the maximum moraine in the Bystra valley, it has been inferred based on geomorphologic evidence, deglaciation chronology of adjacent valleys, ELA position as well as glacier-climate modelling results, that the moraine age is too young and the ridge was likely eroded after deposition. We suggest that the maximum advance in the Bystra Valley occurred most likely during the global LGM as it was shown to be the case in the High Tatra Mountains (Makos et al., 2014; Makos, 2015; Engel et al., 2015).

Two younger recessional stages took place during the LG. They can be correlated with the GS-2.1a (pre- Bølling) and GI-1d (Older Dryas). The horizontal extent of both stages was very similar and they were determined likely by almost uniform climatic conditions. It seems that post-LG1 glacier retreat was controlled mainly by the stronger insolation (higher ablation rates) on the south-facing slopes during the Bølling/Allerød Interstadial.

The LGM glacier advance occurred when the annual temperature was lower than today by about 11–12 °C and precipitation was reduced by 40–60%. These results are in agreement with modelled proxies in the High Tatra Mountains (Makos et al., 2014). The LG1 and LG2 stages were controlled by 10 °C decreased in temperature and about 30% lower precipitation. Such scenario show that during the LG, the accumulation in the Western Tatra Mountains could have been slightly (20–30%) higher than in the eastern part of the massif. The observed diversity and complicated pattern of the precipitation spatial distribution in the Tatra Mountains during the LG is based on a very limited data set at the moment and other palaeoclimatological studies in the massif are strongly needed. Such studies should be also extended into other formerly glaciated areas in the Carpathians. This would give the opportunity to reconstruct the general atmosphere circulation pattern over central Europe during the termination of the last ice age.

Acknowledgements

The project was funded by a grant of the National Science Centre (NCN) (Project No. 2011/03/B/ST10/06188). All fieldwork was undertaken with permission of the Tatra National Park. The French national AMS facility ASTER (CEREGE) is supported by the INSU/CNRS, the French MESR, and the CEA institute. We are grateful to M. Arnold, G. Aumaître, and K. Keddarouche for the AMS measurements.

References

Allen, R., Siegert, M., Payne, A.J., 2008. Reconstructing glacier-based climates of LGM Europe and Russia — part 2: a dataset of LGM precipitation/temperature relations derived from degree-day modeling of paleo glaciers. Clim. Past 4, 249–263.

Balco, G., Briner, J., Finkel, R.C., Rayburn, J.A., Ridge, J.C., Schaefer, J.M., 2009. Regional beryllium-10 production rate calibration for late-glacial northeastern North America. Quat. Geochronol. 4 (2), 93–107.

Ballantyne, C., 1997. Periglacial trimlines in the Scottish Highlands. Quat. Int. 38/39, 119–136.

Ballantyne, C.K., 2010. Extent and deglacial chronology of the last British–Irish Ice sheet: implications of exposure dating using cosmogenic isotopes. J. Quat. Sci. 25, 515–534.

Baumgart-Kotarba, M., Kotarba, A., 1997. Würm glaciation in the Biała Woda Valley, High Tatra Mountains. Stud. Geomorphol. Carpatho-Balc. 31, 57–81.

Björck, S., Walker, M.J.C., Cwynar, L.C., Johnsen, S., Knudsen, K.-L., Lowe, J.J., Wohlfarth, B., INTIMATE Members, 1998. An event stratigraphy for the last termination in the North Atlantic region based on the Greenland ice-core record: a proposal by the INTIMATE group. J. Quat. Sci. 13, 283–292.

Braithwaite, R.J., 1995. Positive degree-day factors for ablation on the Greenland ice sheet studied by energy-balance. J. Glaciol. 41, 153–160.

Braithwaite, R.J., Zhang, Y., 2000. Sensitivity of mass balance of five Swiss glaciers to temperature changes assessed by tuning a degree-day model. J. Glaciol. 46, 7–14.

Brocklehurst, S.H., Whipple, K.X., Foster, D., 2008. Ice thickness and topographic relief in glaciated landscapes of the western USA. Geomorphology 97, 35–51.

Broecker, W.S., 2006. Was the YD triggered by a flood? Science 312, 1146–1148.

Budd, W.F., Keage, P.L., Blundy, N.A., 1979. Empirical studies of ice sliding. J. Glaciol. 23, 157–170.

Chmeleff, J., von Blanckenburg, F., Kossert, K., Jakob, D., 2010. Determination of the ^{10}Be half-life by multicollector ICP-MS and liquid scintillation counting. Nucl. Instr. Meth. B 263 (2), 192–199.

Clark, P.U., Dyke, A.S., Shakun, J.D., Carlson, A.E., Clark, J., Wohlfarth, B., Mitrovica, J.X., Hostetler, S.W., McCabe, M., 2009. The last glacial maximum. Science 325, 710–714.

Darnault, R., Rolland, Y., Braucher, R., Bourlès, D., Revel, M., Sanchez, G., Bouissou, S., 2012. Timing of the last deglaciation revealed by receding glaciers at the Alpine-scale: impact on mountain geomorphology. Quat. Sci. Rev. 31, 127–142.
Delmas, M., 2015. The last maximum ice extent and subsequent deglaciation of the Pyrenees: an overview of recent research. Cuad. Investig. Geogr. 41 (2), 359–408.
Delmas, M., Calvet, M., Gunnell, Y., Braucher, R., Bourlès, D., 2011. Palaeogeography and ^{10}Be exposure-age chronology of Middle and Late Pleistocene glacier systems in the northern Pyrenees: implications for reconstructing regional palaeoclimates. Palaeogeogr. Palaeoclimatol. Palaeoecol. 305, 109–122.
Delmas, M., Gunnell, Y., Braucher, R., Calvet, M., Bourlès, D., 2008. Exposure ages chronology of the last glaciation in the eastern Pyrenees. Quat. Res. 69, 231–241.
Desilets, D., Zreda, M., Prabu, T., 2006. Extended scaling factors for in situ cosmogenic nuclides: new measurements at low latitude. Earth Planet. Sci. Lett. 246, 265–276.
Dunai, T.J., 2001. Reply to comment on 'scaling factors for production rates of in situ produced cosmogenic nuclides: a critical reevaluation' by Darin Desilets, Marek Zreda and Nathaniel Lifton. Earth Planet. Sci. Lett. 188, 289–298.
Dzierzek, J., 2009. Paleogeografia wybranych obszarów Polski w czasie ostatniego zlodowacenia. Acta Geogr. Lodz. 95, 1–112.
Dzierzek, J., Nitychoruk, J., Zreda-Gostynska, G., Zreda, M.G., 1999. Metoda datowania kosmogenicznym izotopem ^{36}Cl – nowe dane do chronologii glacjalnej Tatr Wysokich. Przegląd Geol. 11 (47), 987–992.
Engel, Z., Braucher, R., Traczyk, A., Léanni, L., ASTER team, 2014. ^{10}Be exposure age chronology of the last glaciation in the Krkonose Mountains, Central Europe. Geomorphology 206, 107–121.
Engel, Z., Mentlik, P., Braucher, R., Minar, J., Léanni, L., Aster Team, 2015. Geomorphological evidence and ^{10}Be exposure ages for the Last Glacial Maximum and deglaciation of the Velk a and Mala Studena dolina valleys in the High Tatra Mountains, central Europe. Quat. Sci. Rev. 124, 106–123.
Fabel, D., Ballantyne, C.K., Xu, S., 2012. Trimlines, blockfields, mountain-top erratics and the vertical dimensions of the last British-Irish Ice Sheet in NW Scotland. Quat. Sci. Rev. 55, 91–102.
Federici, P.R., Granger, D.E., Ribolini, A., Spagnolo, M., Pappalardo, M., Cyr, A.J., 2012. Last Glacial Maximum and the Gschnitz stadial in the Maritime Alps according to ^{10}Be cosmogenic dating. Boreas 41, 277–291.
Feurdean, A., Klotz, S., Brewer, S., Mosbrugger, V., Tamas, T., Wohlfarth, B., 2008. Lateglacial climate development in NW Romania — comparative results from three quantitative pollen-based methods. Palaeogeogr. Palaeoclimatol. Palaeoecol. 265 (1–2), 121–133.
Gadek, B., 1998. Würm glaciation of Tatra Mountains in light of the selected valley glacier reconstruction based on glaciological conformities. Pr. Nauk. Uniw. Śląskiego w katowicach 1741, 1–151 (in Polish with English summary).
González-Sampériz, P., Valero-Garcés, B.L., Moreno, A., Jalut, G., García-Ruiz, J.M., Martí- Bono, C., Delgado-Huertas, A., Navas, A., Otto, T., Deboubat, J.J., 2006. Climate variability in the Spanish Pyrenees during the last 30,000 yr. revealed by the El Portalet sequence. Quat. Res. 66, 38–52.
Haeberli, W., 1996. Glacier fluctuations and climate change detection. Geogr. Fis. Din. Quaternaria 18, 191–199.
Hemming, S., 2004. Heinrich events: massive Late Pleistocene detritus layers of the North Atlantic and their global climate imprint. Rev. Geophys. 42, 1–43.
Heyman, B.M., Heyman, J., Fickert, T., Harbor, J.M., 2013. Paleo-climate of the central European uplands during the Last Glacial Maximum based on glacier mass-balance modeling. Quat. Res. 79, 49–54.
Heyman, J., 2014. Paleoglaciation of the Tibetan Plateau and surrounding mountains based on exposure ages and ELA depression estimates. Quat. Sci. Rev. 91, 30–41.
Hughes, P.D., Woodward, J.C., van Calsteren, P.C., Thomas, L.E., Adamson, K., 2010. Pleistocene ice caps on the coastal mountains of the Adriatic Sea: palaeoclimatic and wider palaeoenvironmental implications. Quat. Sci. Rev. 29, 3690–3708.
Hughes, P.D., Woodward, J.C., van Calsteren, P.C., Thomas, L.E., 2011. The glacial history of the Dinaric Alps, Montenegro. Quat. Sci. Rev. 30, 3393–3412.
Isarin, R.F.B., Renssen, H., 1999. Reconstructing and modelling Late Weichselian climates: the YD in Europe as a case study. Earth-Science Rev. 48, 1–38.
Ivy-Ochs, S., 2015. Glacier variationsin the European Alps at the end of the last glaciation. Cuad. Investig. Geogr. 41 (2), 295–316.
Ivy-Ochs, S., Kerschner, H., Kubik, P.W., Schlüchter, C., 2006. Glacier response in the European Alps to Heinrich event 1 cooling: the Gschnitz stadial. J. Quat. Sci. 21, 115–130.
Ivy-Ochs, S., Kerschner, H., Maisch, M., Christl, M., Kubik, P.W., Schlüchter, C., 2009. Latest Pleistocene and Holocene glacier variation in the European Alps. Quat. Sci. Rev. 28, 2137–2149.
Ivy-Ochs, S., Kerschner, H., Reuther, A., Preusser, F., Maisch, M., Kubik, P.W., Schlüchter, C., 2008. Chronology of the last glacial cycle in the European Alps. J. Quat. Sci. 23, 559–573.
Jost, A., Lunt, D., Kageyama, M., Abe-Ouchi, A., Peyron, O., Valdes, P.J., Ramstein, G., 2005. High resolution simulations of the last glacial maximum climate over Europe: a solution to discrepancies with continental paleoclimatic reconstructions? Clim. Dyn. 24, 577–590.
Kageyama, M., Lainé, A., Abe-Ouchi, A., Braconnot, P., Cortijo, E., Crucifix, M., de Vernal, A., Guiot, J., Hewitt, C.D., Kitoh, A., Kucera, M., Marti, O., Ohgaito, R., Otto-Bliesner, B., Peltier, W.R., Rosell-Melé, A., Vettoretti, G., Weber, S.L., Yu, Y., 2006. Last Glacial Maximum temperatures over the North Atlantic, Europe and western Siberia: a comparison between PMIP models, MARGO sea-surface temperatures and pollen-based reconstructions. Quat. Sci. Rev. 25, 2082–2102.
Kelly, M., Buoncistriani, J.-F., Schlüchter, C., 2004. A reconstruction of the last glacial maximum (LGM) ice-surface geometry in the western Swiss Alps and contiguous Alpine regions in Italy and France. Eclogae Geol. Helvetiae 97, 57–75.
Kelly, M.A., Ivy-Ochs, S., Kubik, P.W., von Blanckenburg, F., Schlüchter, C., 2006. Exposure ages of glacial erosional features in the Grimsel Pass region, central Swiss Alps. Boreas 35, 634–643.
Kern, Z., Laszlo, P., 2010. Size specific steady-state accumulation area ratio: an improvement for equilibrium line estimation of small paleoglaciers. Quat. Sci. Rev. 29, 2781–2787.
Klimaszewski, M., 1988. Rzeźba Tatr Polskich Warszawa.
Koperowa, W., 1962. The history of the Late-Glacial and Holocene vegetation of the Nowy Targ basin. Acta Paleobot. 11, 1–62 (in Polish with English summary).
Korschinek, G., Bergmaier, A., Faestermann, T., Gerstmann, U.C., Knie, K., Rugel, G., Wallner, A., 2010. A new value for the half-life of ^{10}Be by heavy-ion elastic recoil detection and liquid scintillation counting. Nucl. Instr. Meth. B 268 (2), 187–191.
Křížek, M., Mida, P., 2013. The influence of aspect and altitude on the size, shape and spatial distribution of glacial cirques in the High Tatras (Slovakia, Poland). Geomorphology 198, 57–68.
Kuhlemann, J., Gachev, E., Gikov, A., Nedkov, S., Krumrei, I., Kubik, P., 2013. Glaciation in the Rila mountains (Bulgaria) during the last glacial maximum. Quat. Int. 293, 51–62.
Kuhlemann, J., Milivojevic, M., Krumrei, I., Kubik, P., 2009. Last glaciation of the Sara Range (Balkan Peninsula): increasing dryness from the LGM to the Holocene. Austrian J. Earth Sci. 102, 146–158.
Kuhlemann, J., Rohling, E.J., Krumrei, I., Kubik, P., Ivy-Ochs, S., Kucera, M., 2008. Regional synthesis of Mediterranean circulation during the Last Glacial Maximum. Science 321, 1338–1340.
Kuhn, M., 1984. Mass budget imbalances as criterion for a climatic classification of glaciers. Geogr. Ann. 66A, 229–238.
Kull, C., Grosjean, M., 2000. Late Pleistocene climate conditions in the north Chilean Andes drawn from a climate glacier model. J. Glaciol. 46, 622–632.
Lal, D., 1991. Cosmic ray labeling of erosion surfaces: in situ nuclide production rates and erosion models. Earth Planet. Sci. Lett. 104, 424–439.
Larocque-Tobler, I., Heiri, O., Wehrli, M., 2010. Late Glacial and Holocene temperature changes at Egelsee, Switzerland, reconstructed using subfossil chironomids. J. Paleolimnol. 43 (4), 649–666.
Lifton, N., Sato, T., Dunai, T.J., 2014. Scaling in situ cosmogenic nuclide production rates using analytical approximations to atmospheric cosmic-ray fluxes. Earth Planet. Sci. Lett. 386, 149–160.
Lifton, N.A., Bieber, J.W., Clem, J.M., Duldig, M.L., Evenson, P., Humble, J.E., Pyle, R., 2005. Addressing solar modulation and long-term uncertainties in scaling secondary cosmic rays for in situ cosmogenic nuclide applications. Earth Planet. Sci. Lett. 239, 140–161.
Lindner, L., Dzierżek, J., Marciniak, B., Nitychoruk, J., 2003. Outline of Quaternary glaciations in the Tatra Mountains: their development, age and limits. Geol. Q. 47 (3), 269–280.
Lowe, J.J., Rasmussen, S.O., Bjorck, S., Hoek, W.Z., Steffensen, J.P., Walker, M.J.C., Yu, Z.C., The INTIMATE Group, 2008. Synchronisation of palaeoenvironmental events in the North Atlantic region during the Last Termination: a revised protocol recommended by the INTIMATE group. Quat. Sci. Rev. 27, 6–17.
Makos, M., 2015. Deglaciation of the high Tatra mountains. Cuad. Investig. Geogr. 41 (2), 317–336.
Makos, M., Dzierżek, J., Nitychoruk, J., Zreda, M., 2014. Timing of glacier advances and climate in the High Tatra Mountains (Western Carpathians) during the Last Glacial Maximum. Quat. Res. 82, 1–13.
Makos, M., Nitychoruk, J., 2011. Last glacial maximum climatic conditions in the polish part of the high Tatra Mountains (Western carpathians). Geol. Q. 55, 253–268.
Makos, M., Nitychoruk, J., Zreda, M., 2013a. Deglaciation chronology and paleoclimate of the Pięciu Stawów Polskich/Roztoki Valley, High Tatra Mountains, Western Carpathians since the Last Glacial Maximum, inferred from ^{36}Cl exposure dating and glacier- climate modeling. Quat. Int. 293, 63–78.
Makos, M., Nitychoruk, J., Zreda, M., 2013b. The Younger Dryas climatic conditions in the Za Mnichem Valley (Polish High Tatra Mountains) based on exposure-age dating and glacier-climate modeling. Boreas 42 (3), 745–761.
Mentlik, P., Engel, Z., Braucher, R., Léanni, L., Team, Aster, 2013. Chronology of the late Weichselian glaciation in the Bohemian Forest in Central Europe. Quat. Sci. Rev. 65, 120–128.
Niedźwiedź, T., 1992. Climate of the Tatra Mountains. Mt. Res. Dev. 12, 131–146.
Nishiizumi, K., Imamura, M., Caffee, M.W., Southon, J.R., Finkel, R.C., McAninch, J., 2007. Absolute calibration of ^{10}Be AMS standards. Nucl. Instrum. Methods Phys. Res. B 258, 403–413.
Nishiizumi, K., Winterer, E.L., Kohl, C.P., Klein, J., Middleton, R., Lal, D., Arnold, J.R., 1989. Cosmic ray production rates of ^{10}Be and ^{26}Al in quartz from glacially polished rocks. J. Geophys. Res. 94, 17,907–917,915.
Ohmura, A., Kasser, P., Funk, M., 1992. Climate at the equilibrium line of glaciers. J. Glaciol. 38 (130), 397–411.
Palacios, D., Gomez-Ortiz, A., Nuria, A., Vazquez-Selem, L., Salvador-Franch, S., Oliva, M., 2015. Maximum extent of Late Pleistocene glaciers and last deglaciation of La Cerdanya mountains, Southeastern Pyrenees. Geomorphology 231, 116–129.
Pallàs, R., Rodés, A., Braucher, R., Carcaillet, J., Ortuño, M., Bordonau, J., Bourlès, D., Vilaplana, J.M., Masana, E., Santanach, P., 2006. Late Pleistocene and Holocene glaciation in the Pyrenees: a critical review and new evidence from ^{10}Be

exposure ages, south-central Pyrenees. Quat. Sci. Rev. 25, 2937–2963.
Paterson, W.S.B., 1994. The Physics of Glaciers, third ed. Elsevier, Oxford.
Peltier, W.R., Fairbanks, R.G., 2006. Global glacial ice volume and Last Glacial Maximum duration from an extended Barbados sea level record. Quat. Sci. Rev. 25, 3322–3337.
Putkonen, J., Connolly, J., Orloff, T., 2008. Landscape evolution degrades the geologic signature of past glaciations. Geomorphology 97 (1–2), 208–217.
Putkonen, J., Swanson, T., 2003. Accuracy of cosmogenic ages for moraines. Quat. Res. 59 (2), 255–261.
Rasmussen, S.O., Bigler, M., Blockley, S., Blunier, T., Buchardt, B., Clausen, H., Cvijanovic, I., Dahl-Jensen, D., Johnsen, S., Fischer, H., Gkinis, V., Guillevic, M., Hoek, W., Lowe, J., Pedro, J., Popp, T., Seierstad, I., Steffensen, J., Svensson, A., Vallelonga, P., Vinther, B., Walker, M., Wheatley, J.J., Winstrup, M., 2014. A stratigraphic framework for abrupt climatic changes during the Last Glacial period based on three synchronized Greenland ice-core records: refining and extending the INTIMATE event stratigraphy. Quat. Sci. Rev. 106, 14–28.
Reitner, J., 2007. Glacial dynamics at the beginning of Termination 1 in the Eastern Alps and their stratigraphic implications. Quat. Int. 164–165, 64–84.
Renssen, H., Isarin, R.F.B., 2001. The two major warming phases of the last deglaciation at ~14.7 and ~11.5 ka cal BP in Europe: climate reconstructions and AGCM experiments. Glob. Planet. Change 30 (1–2), 117–153.
Reuther, A., Urdea, P., Geiger, C., Ivy-Ochs, S., Niller, H.-P., Kubik, P.W., Heine, K., 2007. Late Pleistocene glacial chronology of the Pietrele Valley, Retezat Mountains, Southern Carpathians constrained by ^{10}Be exposure ages and pedological investigations. Quat. Int. 164–165, 151–169.
Rinterknecht, V., Matoshko, A., Gorokhowich, Y., Fabel, D., Xu, S., 2012. Expression of the Younger Dryas cold event in the Carpathian Mountains, Ukraine? Quat. Sci. Rev. 39, 106–114.
Ruszkiczay-Rüdiger, Z., Kern, L., 2016. Permafrost or seasonal frost? A review of paleoclimate proxies of the last glacial cycle in the East Central European lowlands. Quat. Int. (in press).
Ruszkiczay-Rüdiger, Z., Kern, Z., Urdea, P., Braucher, R., Balazs, M., Schimmelpfennig, I., ASTER Team, 2016. Revised deglaciation history of the Pietrele-Stanisoara glacial complex, Retezat Mts, southern carpathians, Romania. Quat. Int. (in press).
Sarikaya, M.,A., Ciner, A., Haybat, H., Zreda, M., 2014. An early advance of glaciers on Mount Akdağ, SW Turkey, before the global Last Glacial Maximum; insights from cosmogenic nuclides and glacier modeling. Quat. Sci. Rev. 88, 96–109.
Sarikaya, M.A., Zreda, M., Ciner, A., 2009. Glaciations and paleoclimate of Mount Erciyes, central Turkey, since the Last Glacial Maximum, inferred from ^{36}Cl cosmogenic dating and glacier modeling. Quat. Sci. Rev. 28, 2326–2341.
Sarikaya, M.A., Zreda, M., Çiner, A., Zweck, C., 2008. Cold and wet Last Glacial Maximum on Mount Sandıras, SW Turkey, inferred from cosmogenic dating and glacier modeling. Quat. Sci. Rev. 27, 769–780.
Small, D., Rinterknecht, V., Austin, W., Fabel, D., Miguens-Rodriguez, M., Xu, S., 2012. In-Situ cosmogenic exposure ages from the Isle of Skye, North West Scotland-Implications for the timing of deglaciation and readvance from 15-11 ka. J. Quat. Sci. 27, 150–158.
Stone, J., 2000. Air pressure and cosmogenic isotope production. J. Geophys. Res. 105, 23753–23759.
Strandberg, G., Brandefelt, J., Kjellström, E., Smith, B., 2011. High-resolution regional simulation of the last glacial maximum climate in Europe. Tellus 63A, 107–125.
Stroeven, A.P., Heyman, J., Fabel, D., Björck, S., Caffee, M.W., Fredin, O., Harbor, J.M., 2015. A new Scandinavian reference ^{10}Be production rate. Quat. Geochronol. 29, 104–115.
Taylor, J.R., 1997. An Introduction to Error Analysis. University Science Books, Sausalito, CA.
Wilson, P., Schnabel, Ch, Wilcken, K., Vincent, P., 2013. Surface exposure dating (^{36}Cl and ^{10}Be) of post-Last Glacial Maximum valley moraines, Lake District, northwest England: some issues and implications. J. Quat. Sci. 4, 379–390.
Zasadni, J., Kłapyta, P., 2014. The Tatra Mountains during the last glacial maximum. J. Maps 10 (3), 440–456.
Żarnowski, M., 2015. Deglacjacja Doliny Bystrej w Tatrach Zachodnich (master thesis – in Polish with English abstract). Archiwum IGP, Uniwersytet Warszawski, pp. 1–144.